DEP Agreement No.:	**MICCI Project 28 Phase 2**		
Grantee Name:	Florida Atlantic University		
Grantee Address:	5600 US-1 N, Ft. Pierce, FL 34946		
Grantee's Grant Manager:	Dr. Jordon Beckler	**Telephone No.:**	772-242-2421
		(cell)	404-594-0293

Reporting Period: **Final Report,** Period of Performance 2/15/23 – 8/15/23

Project Number and Title: Methods Comparison for ISO 7027 - Kristin Jacobs Coral Reef Ecosystem Conservation Area, Martin County: MICCI Project 28 Phase 2

Authored by:

Florida Atlantic University:
Jordon Beckler (PI)
Owen Silvera (Graduate student)

This report is submitted in accordance with the reporting requirements of DEP Agreement No. MICCI Project 28 Phase 2 and accurately reflects the activities associated with the project.

9/28/23

Table of Contents

Summary

No formal comparison study has previously been conducted for instruments measuring turbidity in Florida nearshore or coastal waters. Most in situ, continuous, turbidity loggers are not compliant with the current DEP field turbidity protocol (FT1600), which follows EPA Method 180.1 and measures light scattering in the visible range. There are many instruments that are capable of continuously measuring and monitoring turbidity that are compliant with a different method, ISO 7027, which operates in the near-infrared range. For DEP to utilize data from these instruments for the purpose of establishing background turbidity, assessing water quality standards attainment, or permit compliance monitoring, data obtained from turbidity measurements in accordance with FT1600/EPA 180.1 must be compared with data collected by an ISO 7027-compliant instrument conducted in accordance with an Alternative Methods Approval. A series of comparative measurements was therefore designed to test the utility of the ISO 7027 method for routine environmental monitoring in the Kristin Jacobs Coral Reef Ecosystem Conservation Area (ECA) and nearby waters. Goals included: 1) Compare 60 natural samples subject to EPA 180.1 and ISO 7027 turbidity measurements immediately after collection, after a delay of 24-48 hours and finally, using an ISO 7027 sensor operated in situ. This would serve as the primary methods comparison; 2) Determine the degree that these proxy measurements could yield Total Suspended Solids (TSS), a major variable of interest for coral reef health; and 3) evaluate potential interferences affecting turbidity measurements that could potentially explain deviations between EPA 180.1 and ISO 7027 results.

This study found that EPA 180.1 and ISO 7027 sensors are highly comparable over a wide range of turbidity values indicated by results of pair-wise t-tests and linear regressions, the latter returning R^2 values >0.9 in the range of turbidity values from 0-30 (NTU/FNU). There were no significant differences between groupings. Despite the results of t-tests, however, the coefficients of regression lines relating ISO 7027 to EPA 180.1 consistently deviated from a 1:1 response, with the ISO 7027 method consistently reporting higher values (~22%) relative to the EPA 180.1 method, likely due to water color interference experienced with the EPA 180.1 method. Interestingly, absolutely no correlation between any turbidity method group and TSS was observed, suggesting alternative instrumentation should be employed if TSS is the desired target.

Overall, we recommend that DEP incorporate continuous ISO 7027 turbidity monitoring technology used regularly in scientific research and industry into its SOPs; however, an empirical correction scheme should be employed to ensure best compatibility with existing EPA 180.1 data. We provide a protocol for implementing an empirical correction to ISO 7027 data, using only water temperature to align magnitudes of EPA 180.1 and ISO 7027 method results to be within 4% over the turbidity range found in this study (0-30 NTU). Furthermore, this project lays the groundwork for incorporating historical and new ISO 7027 instrument data into WIN, overall increasing our understanding of background turbidity in the ECA. Data collected during this project and historical projects in which turbidity was monitored could also supplement DEP's Division of Environmental Assessment and Restoration's (DEAR) triennial review process and overall, the modification of the turbidity criterion (FAC 62-302). Finally, we propose a future study to better understand the relationships between turbidity, TSS, and light transmission as it relates to benthic health.

Introduction

Background

Turbidity data used to monitor compliance during marine construction (see Section 10.2.4 of Applicants Handbook Volume 1 and Florida Administrative Code [FAC] 32-330.301) or to define background turbidity (FAC 62-302) in state waters must be collected in accordance with Department of Environmental Protection (DEP) Standard Operating Procedure (SOP) FT1600 (FDEP 2017). This is generally limited to discrete sampling. The full extent to which turbidity fluctuates may be underestimated using FT1600, especially if that sampling is conducted several hours, days or weeks apart. The objective of Phase 1 of the Maritime Industry and Coastal Construction Impacts (MICCI) Local Action Strategy Project #28 (MICCI 28) was to obtain all available turbidity data sets collected in the ECA. Phase 1 indicated only one long-term turbidity data set in the ECA, which is being conducted by CRCP. Turbidity data from this study spans over 5 years of monthly sampling at various locations in the Kristin Jacobs Coral Reef Ecosystem Conservation Area (ECA) and is compliant with FT1600. While this provides a spatially broad data set, monthly sampling most likely does not capture short- and long-term changes in turbidity and suspended sediment during natural and anthropogenic disturbances.

Most in situ, continuous, turbidity loggers are not compliant with the current DEP field turbidity protocol (FT1600), which follows EPA Method 180.1 (EPA 180.1) (U.S. EPA, 1993) and measures light scattering in the visible range. There are many instruments that are capable of continuously measuring and monitoring turbidity that are compliant with a different method: International Organization for Standardization (ISO) Method 7027 (ISO 7027) (ISO, 2016). ISO 7027 measures scattering in the near-infrared range (NIR). The latter method is used internationally and employed by most continuous sensors that could be used for routine in situ water quality assessment in the ECA. The advantage of using a NIR light source in place of a white light source is that interference caused by either the color of suspended particulates or dissolved material (e.g., colored dissolved organic matter [CDOM]) is minimized. Additionally, in situ turbidity sensors are commonly configured with NIR light sources and unlike discrete EPA 180.1 measurements, these ISO 7027 sensors are capable of capturing short- and long-term changes in turbidity and suspended sediment from natural and anthropogenic disturbances. In contrast, turbidity measured in colored water samples using nephelometric methods specifying a white light source (e.g., EPA 180.1) may be negatively biased and can thus underestimate the actual turbidity level (Sadar, 2004). Continuous ISO 7027 sensors could provide more temporal information for a particular water body and an improved understanding of background turbidity in different areas of the ECA, especially in areas where turbidity is expected to change due to anthropogenic disturbances over an extended period. Finally, in situ measurement via ISO 7027 also alleviates the requirement of removing samples from the natural environment per EPA 180.1, potentially limiting artifacts due to particle (dis)aggregation, color changes in the presence of sunlight, and contamination. Therefore, the ECA (and potentially other regions of Florida's Coral Reef) could benefit from the use of a broader range of instruments that monitor turbidity or suspended sediment in a continuous manner using a NIR light source. ISO 7027 instruments could also be used for compliance monitoring of DEP's water quality standards (i.e., turbidity shall not exceed 29 NTU above background) during construction projects like beach nourishment and dredging.

For DEP to utilize data from these instruments for the purpose of establishing background turbidity, assessing water quality standards attainment, or permit compliance monitoring, data obtained from turbidity measurements in accordance with FT1600 (e.g., EPA 180.1) must be compared with data collected by an instrument compliant with ISO 7027. This comparison must be conducted in accordance with an Alternative Methods Approval (See FA 2200, Review and Approval of Alternative Procedures in FA1000), which is the primary purpose of the present study. Although both methods involve sensors which are attempting to quantify suspended particulate matter (SPM), they are often non-predictively related to SPM measured through direct methods like suspended sediment concentration and total suspended solids (TSS). However, both the EPA 180.1 and ISO 7027 turbidity methods stipulate that sensors are calibrated, similarly, using a colloidal solution of formazin. Both EPA and ISO methods quantify the scatter of incident light at a right angle, while the EPA 180.1 method specifies that the incident light is in the wavelength range 400-600 nm whereas the ISO method specifies that the incident light lies in the NIR wavelength range (i.e., 700-900 nm).

Finally, to completely integrate the ISO 7027 method, its relationships with the EPA 180.1 method must be clarified in all use cases, i.e., in situ, field, and delayed measurements (given that the EPA 180.1 measurements are acceptable if measurements are conducted within 48 hours of sample collection). It is not known if ISO 7027 yields equivalent results to EPA 180.1 after a similar holding time but given that 1) multiple laboratory ISO 7027 systems are commercially available, and 2) challenging field conditions may necessitate delayed analyses, this flexibility could be beneficial for future monitoring program implementations. Therefore, this study sought to evaluate whether delayed mode analyses via EPA 180.1 and ISO 7027 techniques yields equivalent results as immediate or in situ analyses.

Moreover, should the relationships between data collected using EPA 180.1 and ISO 7027 methods change depending on when the measurements were conducted (i.e., in situ, field, or delayed), then perhaps ancillary data such as temperature, salinity, water color, or dissolved organic carbon (DOC) could predictively account for and allow correction to ultimately yield a turbidity value that is comparable to EPA 180.1 measurements. While interferences are documented for EPA 180.1 and ISO 7027 (U.S. EPA, 1993; ISO, 2016), an understanding of the extent that these interferences are present in Florida-based samples is desirable for evaluating the utility of existing and future collected datasets, as well as for informing sensor selection for future studies as a function of expected field conditions (i.e., marine vs. estuary). This information may provide for additional confidence when comparing – and perhaps noting significant deviations between – datasets collected by either or both types of measurements. A suite of interferences should thus be measured and evaluated with respect to any relative effects on the EPA 180.1 and ISO 7027-retrieved turbidities.

Optical behavior of particulates in a water matrix are subject to numerous (light) band-specific interferences in the visible to NIR range which can affect light absorption and scattering and thus turbidity measurement, and ultimately the derivation of desired proxy targets (i.e., SPM). In particular, the reliance of scatter at 90˚ in turbidity methods is subject to negative bias by absorbing constituents in water which diminish scattered light reaching the detector. Salinity and temperature impart optical effects which are maximal in the NIR region (Sullivan et al., 2006). Furthermore, the effects of both salt (absorption ~10^{-4} m^{-1} PSU) and temperature (absorption ~10^{-2} m^{-1} $°C^{-1}$) are variable but expected to be relatively minor; however, temperature may contribute a larger overall bias, considering the denominator bases (PSU and °C) likely vary over the same order within the ECA. Water color in filtered samples is primarily

controlled by absorption due to CDOM. CDOM likely impart a significant negative bias on EPA 180.1 measurement because visible water absorption by CDOM in coastal/estuarine systems can range from 0.1-10 m^{-1} (Kirk, 1994), potentially affecting absorption up to several orders of magnitude more than either salt or temperature. The ISO 7027 sensor should not suffer similar interferences, however, because absorption by CDOM is typically unappreciable in the NIR range. While Dissolved Organic Carbon (DOC) is commonly considered to be the most important dissolved light-absorbing component in natural waters, recent research has demonstrated that water color in estuaries draining organic-rich watersheds can also be largely regulated by dissolved iron (dFe) (Logozzo et al., 2022). The complexation of dFe by DOC is known to enhance the absorption of the pool of CDOM (Xiao et al., 2013). Our own ongoing work demonstrates that dFe concentrations within the St. Lucie Estuary can increase approximately 10-fold after periods of intense discharge, probably due to the reductive release of iron/DOC from waterlogged and chemically reducing soils (Beckler, unpublished). During these periods, water color, analyzed using EPA method 2120-C and reported in units of CU, correlates much more closely with dFe than DOC. We therefore expected that the respective concentrations of these two analytes could explain deviations between EPA 180.1 and ISO 7027, given the sensitivity of the former method to light-absorbing chemical components in the visible range. These effects may be particularly pronounced offshore (in the ECA), where estuarine-derived particulates may have sedimented but plume-entrained DOC/dFe may remain in solution.

Project Goals

To the knowledge of DEP's Coral Reef Conservation Program (CRCP), no comparison study has been conducted for instruments measuring turbidity in Florida nearshore or coastal waters. A series of comparative measurements was therefore designed to test the utility of the ISO 7027 method for routine environmental monitoring in the ECA and nearby waters. This work was grouped into three objectives:

1. The primary objective of this work was to compare measurements recorded in situ via an ISO 7027 probe with those measured with EPA 180.1 immediately upon sample collection, and compare both types of measurements to TSS (the primary water quality variable of interest that both are essentially intended to measure).
2. Conduct turbidity measurements with both instruments again, but with overnight sample storage to simulate potential real-world logistical limitations in which immediate analyses is not possible.
3. Evaluate potential interferences and dependencies of both methods.

Methods

Sample Collection and Immediate Analyses

A more detailed sampling and analyses protocol is described in the Scope of Work. All samples were collected by the field contractor (Florida Atlantic University Harbor Branch) at three St. Lucie Estuary (SLE) and seven ECA sites (Figure 1) at both surface and depth, repeated during each of three sampling surveys. The Sampling Surveys were conducted on 04/21/2023, 05/10/2023, and 05/11/2023 (herein Survey 1, Survey 2, and Survey 3, respectively). A summary of the five modes of turbidity sampling methods is presented in Table 1. "Surface" samples

comprised the minimum depth required to ensure a complete fill of the horizontal Niskin bottle (~ 50 cm). “Depth” samples were collected approximately 1-2 m from the bottom (based on the research vessel’s depth finder). For each measurement set (i.e., 30 surface and 30 at depth), a Hanna Instruments HI9829 probe (sonde) sensor (ISO 7027 compliant) was affixed to the Niskin bottle with Velcro so that the sensor head was unobstructed. Turbidity, temperature, and salinity were recorded on the HI9829 at the appropriate depth and the Niskin bottle was triggered at the same time. Upon retrieval of the Niskin/HI9829 probe, the HI9829 probe was detached from the Niskin bottle. The sample water from the Niskin was transferred to a cuvette for field turbidity analyses via EPA 180.1 using a Hach 2100Q instrument, and a second ISO 7027 turbidity and temperature measurement was conducted using the HI9829 in a 1-L wide-mouth LDPE bottle filled directly from the Niskin. Measurements were obtained within 15 minutes of sample collection. Two additional sets of 1-L wide mouth LDPE bottles filled from the Niskin were also preserved (i.e., placed on ice) for delayed laboratory analyses, described below.

Delayed Sample Processing and Analyses

Methods details for delayed turbidity (Table 1) and supplementary analytes, including TSS (Table 2) are provided below. Upon return to the laboratory after each Sampling Survey, one of the 1-L bottles from each sample location was briefly opened and processed for analyses of supplemental analytes (described in more detail below) by pouring from the bottle into a syringe filtration system, and then this bottle was resealed and placed back in the cooler for delayed mode (next day) turbidity analyses. The second set of collected bottles remained permanently sealed and was shipped/driven to Tritech Laboratories for TSS analyses.

Supplemental sampling and analyses of TSS and potential interferences is summarized in Table 2. The 1-L sample was homogenized by gently swirling the bottle and ~40 mL of sample was poured into the back of a 60 mL polypropylene syringe, which was passed off to a second staff member to filter through acid-rinsed 200 nm pore size polyethersulfone (PES) syringe membranes for subsequent processing and analyses of interferences (i.e., water color, DOC, and dFe). Filtrate for water color was stored temporarily in 15 mL LDPE bottles prior to analysis within 1-2 hours. Filtrate for DOC was directly added, from the syringe/syringe filter membrane, into 24 mL pre-combusted borosilicate glass vials. Filtrate for dFe was stored in 15 mL graduated polypropylene tubes pre-filled with stabilizing reagents. Analysis of dFe was conducted the next day, after allowing the samples to react overnight. During this reaction period, Fe(III) is reduced by hydroxylamine to Fe(II), which is then measured to yield a “total dissolved iron” measurement. The DOC sample vials were frozen until analyses within 30 days.

Delayed-mode turbidity analysis was conducted using the remaining sample in the 1-L bottle that was used for filtering/processing for potential interferences (Table 2). For Surveys 1 and 3 the delayed analysis was performed within 24 hours, and for Survey 2 within 48 hours. Similar to the field procedure, samples were first homogenized and poured directly into the cuvette for EPA 180.1 measurement, and then the HI9829 probe was inserted into the same 1-L bottle to obtain the ISO 7027 and temperature measurement. The second set of 1-L bottles for TSS were shipped overnight or driven to the contracted NELAC certified lab (Tritech Laboratories, DOH ID 83294) on the day of delayed analysis, where TSS analyses occurred within 7 days of collection per the SM2450D method.

Table 1. Turbidity measurements by collection method, sensor configuration, and analysis location.

Analysis Location	Analyte	Collection & processing Method	Analysis procedure	Preservation/ Analyses Method	Sensor Specifications	Derived Units	Measurement label/ID for statistical analyses
Field	Turbidity	Niskin	Dispensed immediately from Niskin to cuvette	FS-1000 FS-2100 FT1000 FT 1600	Hach 2100Q (EPA 180.1)	NTU	Field EPA 180.1 (EPA Field)
Field	Turbidity	Probe mounted to Niskin	Measured in situ alongside Field EPA 180.1 water collection	FT-1000 FS-1000 FS-2100 ISO 7027	HI9829 (ISO 7027)	FNU	Field ISO 7027 in situ (ISO In Situ)
Field	Turbidity	Niskin to 1-L bottle	Sensor inserted into 1-L bottle immediately after collection	FT-1000 FS-1000 FS-2100 ISO 7027	HI9829 (ISO 7027)	FNU	Field ISO 7027 Bottle (ISO Field)
Lab (Delayed)	Turbidity	Niskin sample collected and preserved overnight in 1-L bottle	Sub-sample dispensed directly into field portable cuvette system day after collection	FT-1000 FS-1000 FS-2100 FT-1600 with 180.1 for sample holding	Hach 2100Q (EPA 180.1)	NTU	Lab EPA 180.1 bottle delayed (EPA Delay)
Lab (Delayed)	Turbidity	Niskin sample collected and preserved overnight in 1-L bottle	Sensor inserted into 1-L bottle	FT-1000 FS-1000 FS-2100 ISO 7027	HI9829 (ISO 7027)	FNU	Lab ISO 7027 bottle delayed (ISO Delay)

Table 2. Breakdown of supplementary analyses performed. Importantly, all supplementary analytes are collected, processed, and analyzed by the FAU laboratory with the exception of TSS, for which samples were processed and analyzed by a contracted NELAC certified laboratory (Tritech Laboratories).

Analysis Location	Analyte	Collection & Processing Method	Analysis procedure	Preservation/ Analyses Method	Sensor / Method Specifications	Derived Units
NELAC Lab (within 7 days)	Total suspended solids	Collected from Niskin and stored on ice overnight in 1-L bottle, shipped overnight to lab day after field survey	Weighing after filtering and drying	FS-1000 FS-2100	SM 2540D	mg/L
Field	Salinity	Probe mounted to Niskin	In situ measurement simultaneous with Field ISO 7027	FT-1000 FT-1300	HI9829	Unitless
Field & Lab	Temperature	Probe mounted to Niskin or inserted into 1-L bottle	Recorded for each of the three modes of ISO 7027 measurements	FT-1000 FT-1400	HI9829	°C
FAU HBOI Laboratory (not NELAC, variable storage times)	Color	Sub-sampled from 1-L bottle in lab same day as sampling, filtered thru 200 nm PES filter, analyzed immediately	Absorption measured immediately @ 455 nm (calibrated vs Pt/Co)	FS-1000 FS-2100 EPA method 110.3 (2120C in APHA 2013 reference)	1-50 cm pathlength modular spectrophotometer r^2	PCU & absorption units (m^{-1})
FAU HBOI Laboratory (not NELAC, variable storage times)	Dissolved organic carbon	Sub-sampled from 1-L bottle in lab same day as sampling, filtered thru 200 nm PES	Combustion & IR detection	FS-1000 FS-2100 NU-160[1]	Shimadzu TOC-L	mM C

		filter, frozen until analyses				
FAU HBOI Laboratory (not NELAC, variable storage times)	Dissolved Fe	Sub-sampled from 1-L bottle same day as sampling, filtered thru 200 nm PES filter, added to pre-prepared reagent filled tubes	Next day colorimetric – reaction with Ferrozine to form purple complex	FS-1000 FS-2100 FAU SOP 314[1]	1-50 cm pathlength modular spectrophotomer[2]	mM Fe

Results & Discussion

Environmental Context

All meta- and raw data is presented in Appendices 1 and 2, respectively. Figure 1 presents a site map for each survey with EPA field turbidity values that are color mapped on a logarithmic scale. While the focus was on marine ECA sites, the few SLE sites surveyed expand the applicability of this study to estuarine environments while also providing a degree of confidence that sensors were functioning properly, e.g., in the event that our results were questionable due to being near the minimum limit of detection of the turbidity methods. To not skew correlations with these higher turbidities, however, the subsequent analyses are approached by both examining the full dataset but also the marine-only samples separately (sensitized analyses). Nonetheless, the maximum EPA turbidities measured in the three surveys likely exceeds those expected within the ECA under typical conditions. These maxima were accordingly 7.55 NTU for the ECA and 18.1 NTU for the SLE.

Survey 1 was conducted on outgoing tide, Survey 2 on incoming tide, and Survey 3 was closest to peak high tide during collection of ECA samples, and all samples were collected within daylight hours within the window ~0800 to 1630. Accordingly, the average salinity and other freshwater signatures, i.e., high DOC and dFe, decreased in the order of Surveys 1, 2, and then 3 (Table 3). For data interpretation, however, it is important to note that the most inland site within the SLE was changed after Survey 1 due to construction on a bridge within the SLE that prevented access to the site without necessitating multiple boat launches. More elevated turbidities were in turn observed for Surveys 1 and 2 than for Survey 3 (Figure 1). Samples collected were assigned an ID scheme which increased numerically along the EST to ECA transect; this allowed creation of an arbitrary x-axis of sample IDs which represents a longitudinal estuarine gradient showing the diminution of freshwater signatures approaching the ECA (Figure 2). Because of the grid pattern used within the ECA, it is not possible to represent the complete dataset with respect to transect longitude, however.

A surveyed site from within the SLE is shared with the Indian River Lagoon Observing Network (irlon.org; Site SLE-ME). IRLON turbidity was compared with discrete turbidity samples collected during the three surveys (Figure 3). The comparison between the non-standard sensor used by IRLON and discrete samples collected by both the ISO and EPA instruments show good agreement between turbidity sensor configurations. However, the hourly turbidity data provided by IRLON sensor shows that the maximum turbidity recorded *between* our surveys was 68.74 NTU, which is a factor of 7.4 greater than the maximum EPA field turbidity collected at this site during either of the bookending discrete surveys (9.26 NTU). Although IRLON is using a non-standard sensor, the good agreement with our discrete samples from individual surveys yet the large differences in overall turbidity magnitude within a 3-week sample window demonstrates the importance of maintaining continuous in situ measurements by an ISO sensor for characterizing turbidity fluctuations in the ECA. This agreement does suggest that this sensor may be an appropriate choice for further examination as a substitute for the EPA, despite the IRLON sensor being neither EPA nor ISO compliant (FLNTU, Seabird Scientific).

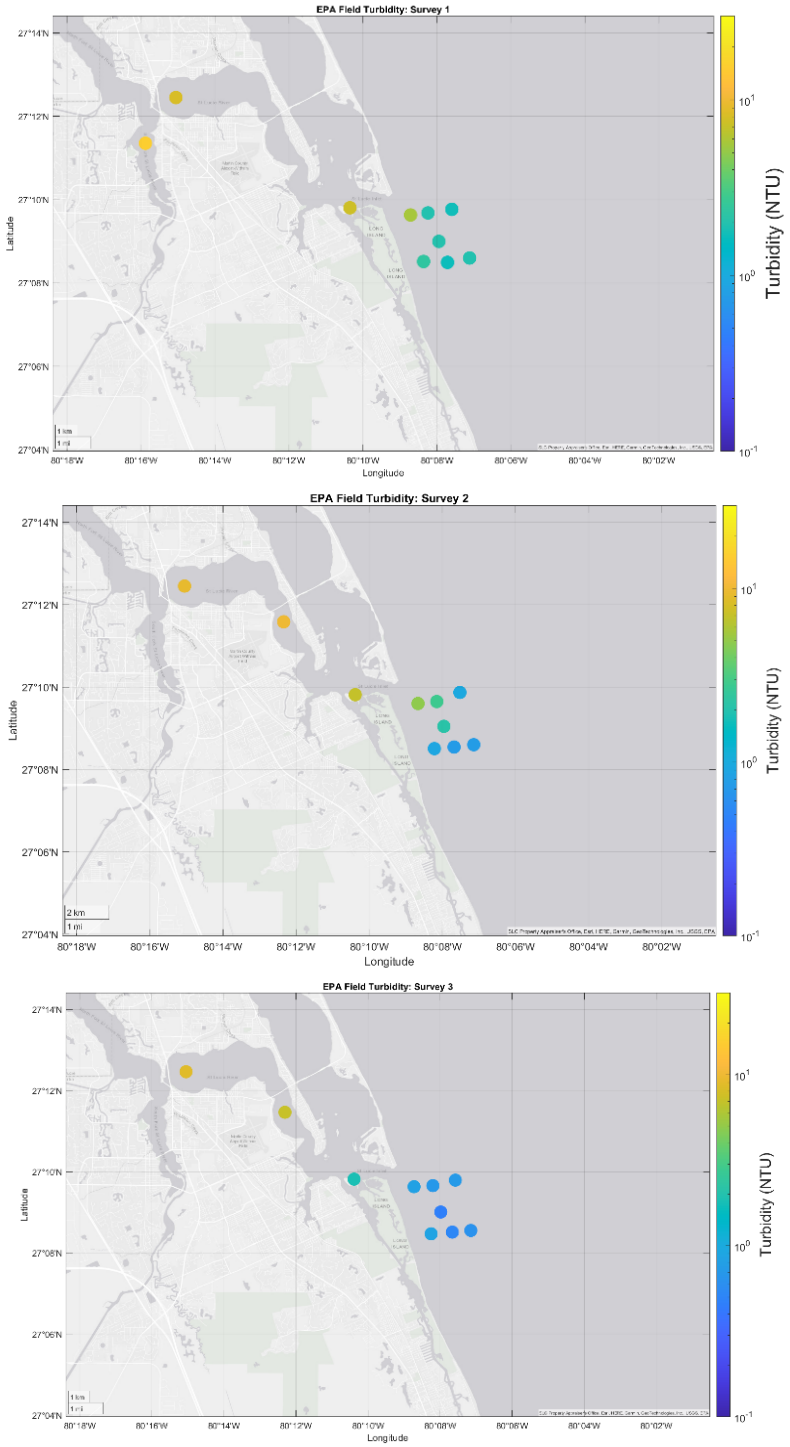

Figure 1. Survey maps of EPA field measured turbidity values (NTU) from the three surveys. Survey 1 was conducted on 04/22/2023 (top), Survey 2 on 05/10/2023 (middle), and Survey 3 (bottom) on 05/11/2023. The EPA Turbidity (NTU) colormap is presented on the logarithmic scale 0.1-30 NTU for all graphics. Site SLE-ME within the SLE was visited each survey and is the second data point from the left in the upper panel. This site was used to compare discrete vs continuous turbidity comparison (see Figure 3).

Table 3. Average values and standard deviations of all measured variables for each survey.

Survey	Salinity (PSU)	EPA Field (NTU)	ISO Field (FNU)	EPA Delay (NTU)	ISO Delay (FNU)	ISO In Situ (FNU)	TSS (mg/L)	Color 412 nm (CU)	DOC (µM)	dFe (µM)
1	31.18 ± 11.54	4.61 ± 4.28	5.81 ± 4.74	4.15 ± 4.00	4.58 ± 4.86	5.49 ± 5.49	40.29 ± 34.33	6.65 ± 13.23	188.1 ± 195.9	0.039 ± 0.042
2	31.33 ± 10.03	4.52 ± 3.89	5.42 ± 4.81	3.69 ± 3.72	4.15 ± 4.30	5.35 ± 4.49	28.17 ± 8.63	10.13 ± 10.97	161.4 ± 139.2	0.033 ± 0.037
3	33.51 ± 9.21	2.24 ± 3.00	2.34 ± 3.46	2.09 ± 2.93	2.4` ± 3.55	2.08 ± 3.46	31.51 ± 9.77	9.77 ± 6.59	96.7 ± 101.9	0.022 ± 0.025

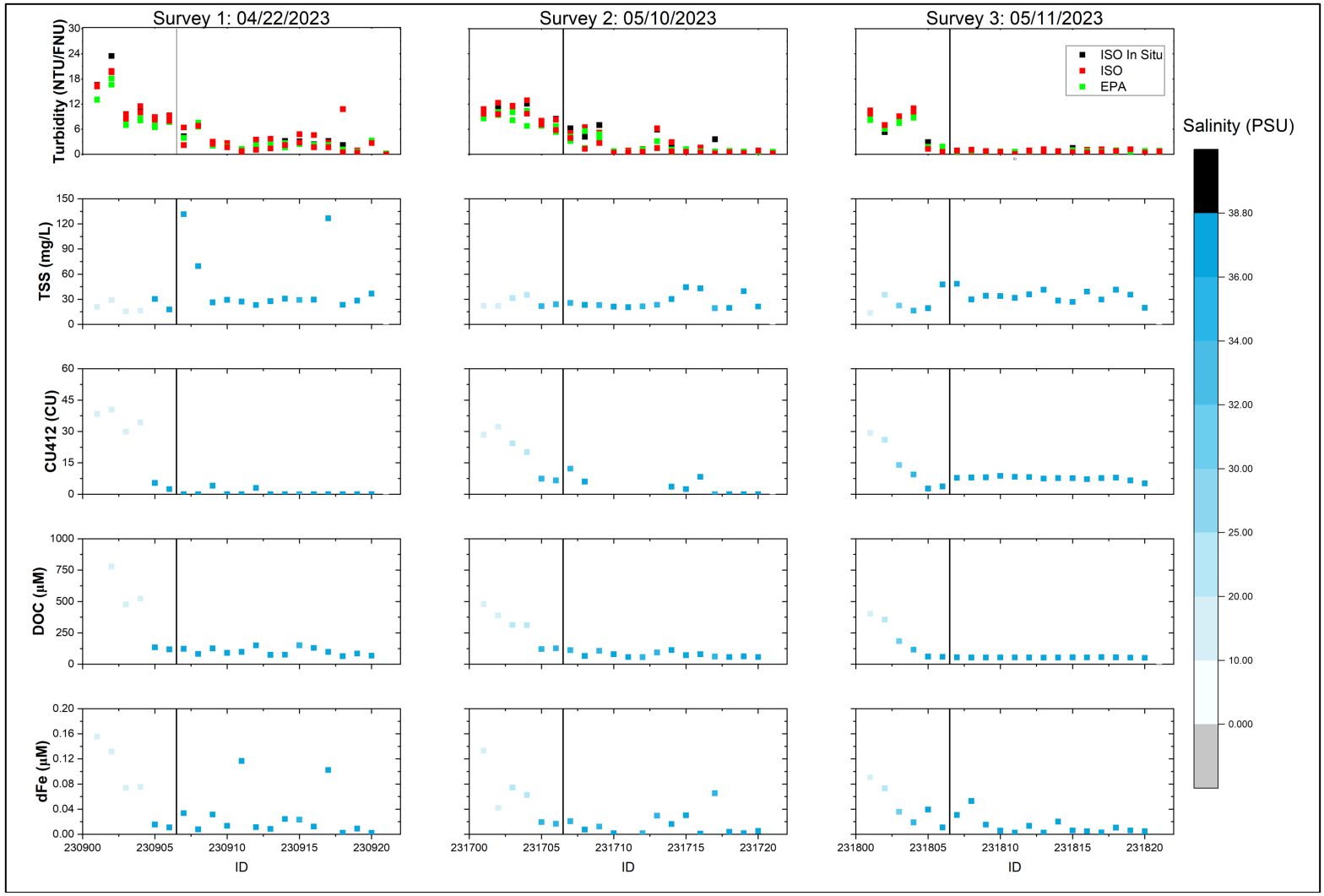

Figure 2. The sample ID scheme increases numerically in the direction of SLE to ECA creating an approximate longitudinal estuarine gradient of freshwater signatures (e.g., DOC & dFe) before the ECA (vertical line). Turbidity is colored according to the grouping (Red: ISO grouped Field and Delay; Green: EPA grouped Field and Delay) while all other supplemental analytes are colored according to salinity.

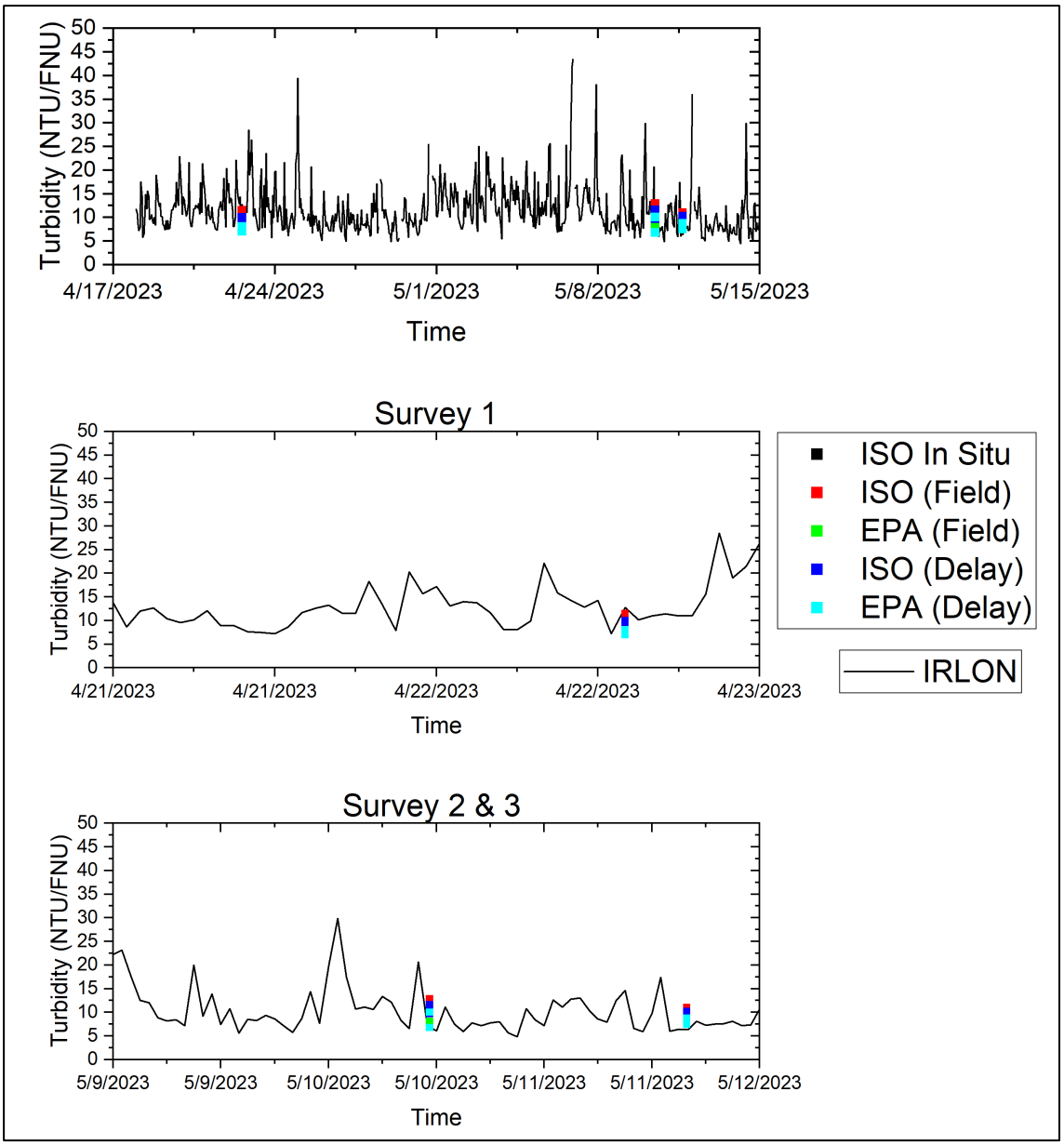

Figure 3. Continuous ISO In Situ turbidity measurement collected by IRLON (line) encompassing the survey window that is superimposed with discrete values of turbidity measured during each survey (points). The entire survey window (top) was confined to Survey 1 (middle) and Surveys 2 and 3 (bottom) for clearer visualization.

Overview of Method Comparability

To determine whether the ISO method serves as an appropriate substitute for the EPA method (i.e., the primary goal of the study), a pairwise t-test was performed on broad groupings. This analysis assessed overall differences between methods (EPA, ISO, ISO In Situ) and analysis location (Field, Delay, and ISO In Situ). For clarification, the ISO In Situ measurement is performed by an ISO instrument but is separated as both a unique analysis technique and location for inter/intra method and location comparisons, as it cannot be replicated by the EPA method.

The first Pairwise-t-test treated turbidity measurements between ISO In Situ, ISO (grouped Field and Delay data), and EPA (grouped Field and Delay data) turbidity measurement groupings. Field and delayed measurements were combined because based on existing turbidity measurement protocols, we are here assuming that no significant differences should present between measurements obtained immediately versus within 48 hours of collection. This analysis shows that the ISO (grouped Field and Delay) and EPA (grouped Field and Delay) measured values of turbidity are not significantly different from each other ($p = 0.55$, Table 4). Furthermore, ISO In Situ turbidity values were not significantly different from EPA (grouped Field and Delay) values ($p = 0.55$) but were more comparable with the ISO (grouped Field and Delay) values ($p = 0.67$). These results show that while the EPA and ISO turbidity values are comparable regardless of whether or not there is a delay in conducting the measurement, some disagreement in data equivalence can be attributed to the nature of the EPA versus the ISO sensor.

Table 4. Pairwise-t-test showing p-values of pairings between ISO, EPA, and ISO In Situ turbidity values which combines field and delayed analyses within the ISO/EPA groups and separates ISO In Situ values (ISO) into a separate group. P-values > 0.05 indicate that there are no significant differences between any method pairings.

Pairwise-t-Test	EPA (grouped Field and Delay)	ISO In Situ
ISO In Situ	0.55	-
ISO (grouped Field and Delay)	0.55	0.67

A second pairwise-t-test was employed to analyze the comparison of analysis location, regardless of method; this test grouped the turbidity measurements irrespective of the method into In Situ, Field, and Delay analyses. In Situ and Field measurements have relatively small differences between the actual timing of sample measurement, while differences between both of those groups and the Delay measurement are greater. Therefore, groups for the second t-test were created to further assess effects of removing samples from the environment and whether analysis time affects this comparison. Results of the second t-test showed that Delay (grouped ISO and EPA) and immediate sample analyses (either grouped EPA Field and ISO Field; or ISO In Situ) do not produce statistically different measurements of turbidity ($p = 0.46$ for both comparisons). However, Delay analyses are overall less comparable with immediately analyzed samples than immediate samples are with themselves, the latter test between Field and In Situ groups indicating the sample sets are more similar ($p = 0.74$, Table 5). These results suggest that delayed

mode analysis may be performed in place of immediate sample analysis if sampling over a large turbidity range (0-30 NTU/FNU), but that immediate analyses yields a small improvement if trying to best match true in situ values.

Statistical analyses were also performed on (sensitized) datasets restricted by the condition EPA Field < 5 NTU (i.e., more typical of the ECA under low flow conditions, see "Sensitivity Analysis" section). This restriction is important to establish the use of the ISO technique for background monitoring in the marine ECA environment, and to ensure that statistical comparisons using the full desensitized range (unrestricted) are not skewed by high turbidity samples, especially given that we are working near the detection limit of the turbidity monitoring techniques. Pairwise t-tests on the sensitized dataset mostly returned results demonstrating statistical equivalence, suggesting comparability between the ISO and EPA configured sensors under high (0-30 NTU/FNU) and low (0-5 NTU/FNU) conditions. However, in the sensitized dataset (EPA Field < 5 NTU) Delay (grouped EPA and ISO) and Field (grouped EPA and ISO) analyses were significantly different from each other ($p = 0.018$) while immediate analyses (i.e., grouped EPA and ISO vs ISO In Situ) were not different ($p = 0.903$; Table 6). Therefore, it may not be advisable to use delayed mode analysis in locations where turbidities naturally occur over a smaller range (e.g., ECA). Overall, for best matchup, sample comparisons should be made with immediately analyzed samples whenever possible during future use of the ISO In Situ measurement technique.

Table 5. Pairwise-t-test showing p-values of analysis location/timing pairings between turbidity values collected in the Field, laboratory (Delay), and In Situ which combines ISO and EPA methods within the Field/Delay groups and then separates In Situ values (ISO) into a separate group. p-values > 0.05 indicate that there are no significant differences between any method pairings.

Pairwise-t-Test	Delay (EPA and ISO)	Field (EPA and ISO)
Field (EPA and ISO)	0.46	-
ISO In Situ	0.46	0.74

Table 6. Pairwise-t-test showing the p-values of a sensitized dataset (i.e., condition = EPA Field < 5 NTU). This analysis is directly comparable with Table 5, except it is performed over a narrower range of turbidity values by the preset condition on the data compared.

Pairwise-t-Test (Sensitized)	Delay (EPA and ISO)	Field (EPA and ISO)
Field (EPA and ISO)	0.02	-
ISO In Situ	0.07	0.90

For the final broad method comparison, turbidity measurements were grouped by both method (EPA and ISO) and analysis location (Field, Delay, and In Situ) so that each individual sample was only represented once, and all measurement types of a given sample could be compared. A pairwise-t-test of this final grouping method showed that there were no significant differences between any of the groups (Table 7). Indeed, decreasing the sample size in each group through increasing specificity resulted in the p-values most indicative of great inter-

method comparability. Furthermore, the only group with evident, albeit non-significant ($p < \sim 1$) differences, was the comparison between EPA Delay and ISO Field mode analyses ($p = 0.79$) which may be a result of combined effects of the different analysis method and analysis location (i.e., time). Nevertheless, this final method comparison in conjunction with the previous pairwise-t-test results from other grouping techniques collectively (Tables 4-7) suggests good comparability between the ISO and EPA methods in several use cases. The summary of use cases compared above were made by ISO In Situ measurements, measurements performed immediately in the field with either EPA or ISO methods, and finally after accounting for delays of up to 48 hours in a laboratory setting. Box plots below (Figure 4) show the minute variability between different groupings tested; this figure further demonstrates that method and location had little effect on turbidity, shown by one-way Analysis of Variance (ANOVA) tests performed on each grouping method which all returned p-values greater than 0.05. A final analysis sought to examine differences in inter-method comparisons between surface and bottom turbidity measurements (Table 8) and found no differences in method comparability based on sample depth.

Table 7. Pairwise-t-test showing p-values of pairings between ISO, EPA, and In Situ turbidity measurements which leave values separated by both method and analysis location. p-values > 0.05 indicate that there are no significant differences between any method pairings.

Pairwise-t-test (All)	EPA Delay	EPA Field	ISO In Situ	ISO Delay
EPA Field	1	-	-	-
ISO In Situ	1	1	-	-
ISO Delay	1	1	1	-
ISO Field	0.79	1	1	1

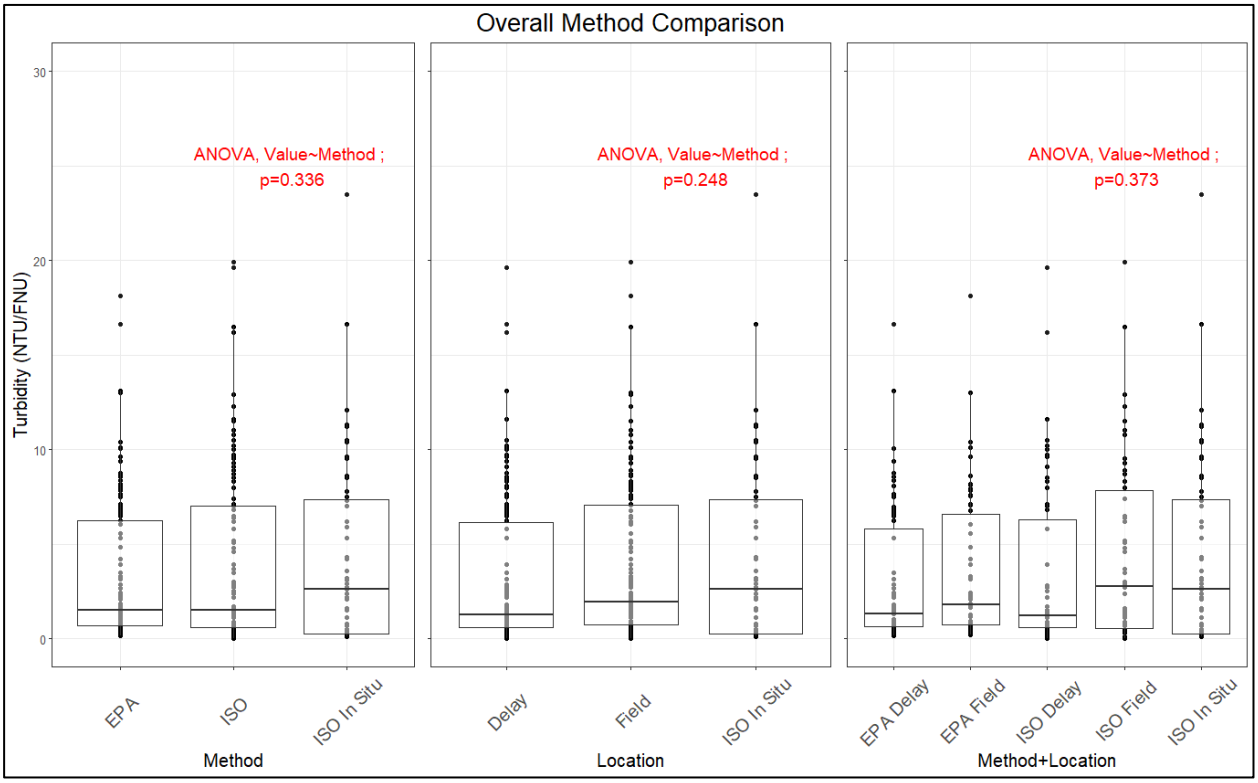

Figure 4. To further confirm results of the pairwise-t-test comparisons between group pairings the same group pairings and respective turbidity values were visualized in the programming language R, where results of one-way ANOVAs are annotated into the graphs. All ANOVAs returned p-values > 0.05 confirming that groups cannot be separated statistically.

Table 8. ANOVA model comparing turbidity measurements by method (e.g., EPA) and Method+Location (e.g. EPA Field) and how these comparison interact with depth (Method:Depth). Overall, the insignificance of both comparisons (i.e., $p > 0.05$) shows that sample depth has no effect on how the two methods compare.

ANOVA	F-Value	p-value
Turbidity~Method:Depth	0.405	0.845
Turbidity~(Method+Location):Depth	0.453	0.905

Modeled Effects of Salinity, Temperature, and CDOM (Full Turbidity Range)

We next determine if matchups between EPA Field measurements with ISO In Situ, ISO Field, and ISO Delay measurements are affected by salinity, temperature, and/or color as covariates. This analysis is intended to provide confidence in emulating the current EPA methodology (FT1600/EPA 180.1) under any future use scenarios of the ISO method, while investigating potential interferences of the comparison. The temperature used was that measured at the ISO location used during analysis; for example, an EPA Field ~ ISO Delay model would use the delayed (laboratory) temperature of the 1-L stored sample in a model. The EPA

measurements were always used as response variables in the models to simulate a situation in which the analyst has ISO turbidity measurements (either ISO In Situ, ISO Field, or ISO Delay) but would like to derive the corresponding EPA measurement. Overall, the regressions of EPA Field vs ISO In Situ, ISO Field, or ISO Delay (with or without additional variables) all had a $R^2 > 0.94$ indicating the goodness of fit between the two methods (Figure 5). However, coefficients (slopes) of each relationship were all between 0.77-0.85, deviating from the expected 1:1 relationship (the ISO method reported higher values than the EPA method, although in actuality, this is likely caused by water color suppressing the EPA sensor response; more on this below).

Furthermore, excluding ISO Delay and just comparing EPA Field with the immediate ISO measurements (i.e., ISO In Situ and ISO Field) the range of coefficients narrows to between 0.77 and 0.82 (Table 9). Finally, salinity had no significant effects on any of the fits between EPA and ISO measurements, whereas temperature had slightly significant ($p < 0.05$) effects which negatively biased ISO measurements in all instances indicated by positive temperature coefficients (0.17-0.25; Table 9). Both salinity and temperature can affect inherent optical properties (IOPs; e.g., scatter) and thus measurements of turbidity; however, temperature effects are two orders of magnitude greater per unit than salinity, i.e., degrees vs PSU. Likely, both salinity and temperature are affecting turbidity, however, salinity on a scale less than the sensitivity of the analysis.

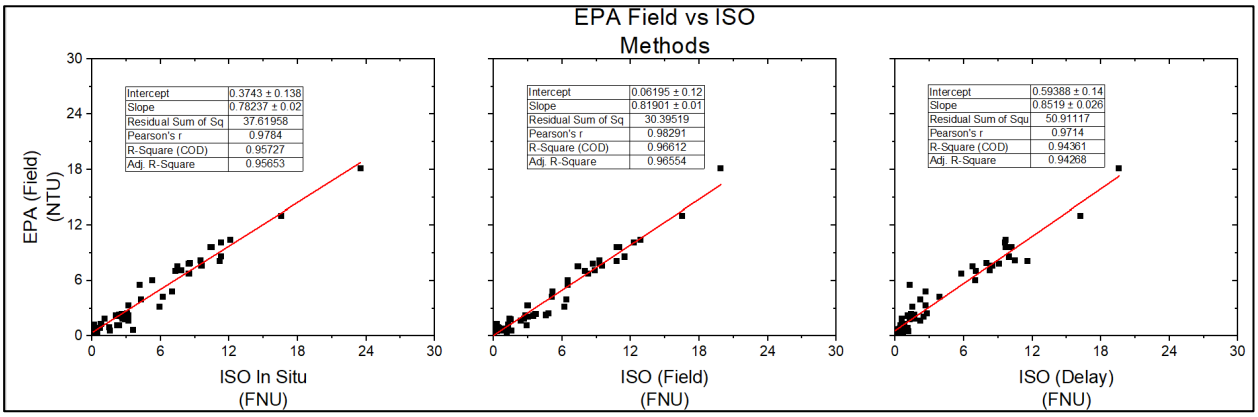

Figure 5. Turbidity covariates comparing EPA Field turbidity values with the three ISO measurement locations, as for Table 9.

Table 9. Multilinear regression models which assess comparability between EPA Field (response) turbidity values to different ISO turbidity values (predictor) collected at different locations/times. Each ISO predictor was assigned an additional covariate of salinity, temperature, or water color at 412 nm to assess whether these water properties affect measurements of turbidity between methods. Coefficients of the ISO predictor (i.e., slopes) and the interfering water property (coefficient 2, when used) are presented alongside the significance of both predictors (p/p2) and the overall goodness of fit of the model (R^2). $p < 0.05$: *; $p < 0.01$: **; $p < 0.001$: ***; $p < 0.0001$: ****

Condition: EPA Field 0-30 NTU	Response: EPA Field				
Independent Variables	Coefficient	Coefficient2	p	p2	R^2
ISO In Situ	0.787	-	****	-	0.957
ISO In Situ + Salinity	0.775	-0.005	****		0.956
ISO In Situ + In Situ Temperature	0.781	0.228	****	*	0.969

ISO In Situ + Color 412	0.783	0.003	****		0.961
ISO Field	0.819	-	****	-	0.966
ISO Field + Salinity	0.813	-0.006	****		0.965
ISO Field + Field Temperature	0.816	0.174	****	*	0.968
ISO Field + Color 412	0.798	0.013	****		0.970
ISO Delay	0.852	-	****	-	0.943
ISO Delay + Salinity	0.879	0.021	****		0.944
ISO Delay + Delay Temperature	0.852	0.245	****	*	0.945
ISO Delay + Color 412	0.901	-0.023	****		0.948

Next, in anticipation of future scenarios where delayed mode analyses are necessary, a comparison of EPA and ISO measurements was conducted on the field samples which were held for 24-48 hours (Table 10). The same mixed models that were used for EPA Field comparisons with the ISO measurements (Table 9) were again used to compare EPA Delay and ISO measurements (Table 10). The range of coefficients expanded (0.663-0.888) and model fits (R^2 = 0.9146-0.99) performed both worse or better when compared to their corresponding EPA Field model fit (i.e. Table 9). The general trends indicate that immediate ISO measurements (both ISO In Situ & ISO Field) were much less comparable to EPA Delay measurements than the ISO Delay measurements (Figure 6). However, for both field and delayed comparisons (Tables 9 & 10), the best fit model was the EPA Delay ~ ISO Delay + $Color_{412}$ model (coef=0.888; R^2=0.99). Interestingly, this model depicts the negative bias (coefficient = -0.03057) of CDOM on the EPA180.1 method using the water color at 412 nm as a measure of CDOM absorption intensity. This finding provides strong evidence that water color is the dominant contributor to differences associated between EPA and ISO methods, particularly when we consider that delayed analyses provide time for processes such as dFe complexation and/or aggregation which may specifically affect color at the wavelength 412 (nm). In the future, a fully exhaustive approach may be undertaken which tests whether the relationship between field measurements of ISO and EPA are dependent on another wavelength, i.e., testing whether the specific wavelength of negative bias on the EPA method is time dependent.

Table 10. Multilinear regression models which assess comparability between EPA Delay (response) turbidity values to different ISO turbidity values (predictor) collected at different locations/times. Each ISO predictor was assigned an additional covariate of salinity, temperature, or water color at 412nm to assess whether these water properties affect measurements of turbidity between methods. Coefficients of the ISO predictor (coefficient) and the interfering water property (coefficient 2) are presented alongside the significance of both predictors (p/p2) and the overall goodness of fit of the model (R^2). $p < 0.05$: *; $p < 0.01$: **; $p < 0.001$: ***; $p < 0.0001$: ****.

Condition: EPA Field 0-30 NTU	Response: EPA Delay				
Independent Variables	Coefficient	Coefficient2	p	p2	R^2
ISO In Situ	0.736		****	-	0.927
ISO In Situ + Salinity	0.663	-0.056	****		0.930
ISO In Situ + In Situ Temperature	0.738	-0.168	****		0.928
ISO In Situ + Color 412	0.712	0.019	****		0.941
ISO Field	0.758		****		0.915
ISO Field + Salinity	0.725	-0.031	****		0.918
ISO Field + Field Temperature	0.761	-0.164	****		0.917
ISO Field + Color 412	0.698	0.036	****		0.928
ISO Delay	0.828		****		0.986
ISO Delay + Salinity	0.833	0.005	****		0.987
ISO Delay + Delay Temperature	0.828	0.068	****		0.986
ISO Delay + Color412	0.888	-0.031	****	***	0.990

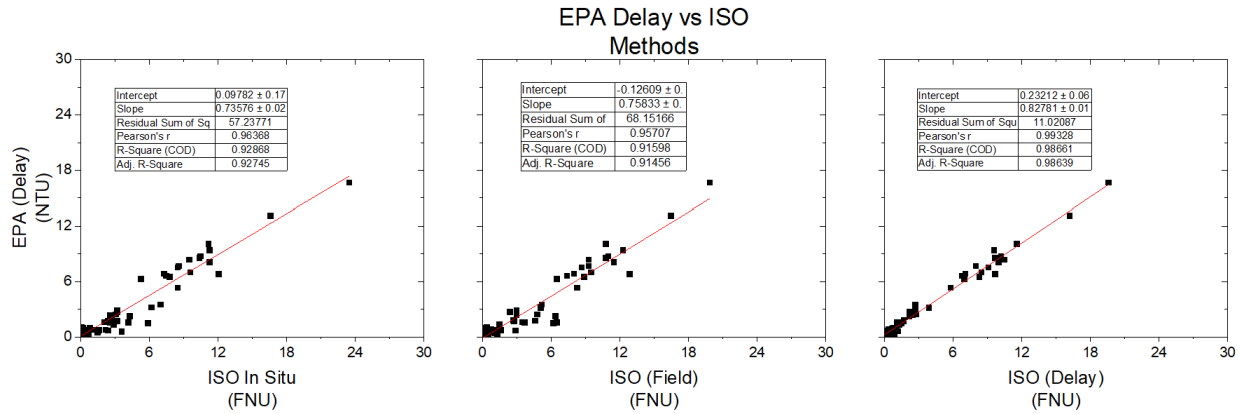

Figure 6. Turbidity covariates comparing EPA Delay turbidity values to the three ISO measurement locations as for Table 10.

Sensitivity Analysis: Modeled Effects of Salinity, Temperature, and CDOM (0-5 NTU)

The set of samples were collected from sites within an estuary and sites in the Coral ECA to expand the range of turbidities (0-30 NTU) during the limited sample period. Long term monitoring projects in the ECA will display a smaller range of turbidities. To exclude non-marine sites, salinities less than 30 PSU were first excluded. Then, the average (2.34 NTU) plus

one standard deviation (2.31 NTU) of the EPA Field measurements were determined to set the maximum range of the turbidity for sensitivity analysis, determined to be ~5 NTU. As the analysis was sensitized to the range typical of normal ECA values (i.e., EPA Field < 5 NTU), relationships between ISO (Delay, Field and In Situ) and EPA Field methods degraded (R^2: 0.68-0.78, Table 11) compared to the same analyses performed on the full range of turbidities (Tables 9). Also, for immediate ISO analyses (either ISO In Situ or ISO Delay), the coefficients decreased from the initial range of 0.77-0.82 to a new range of 0.51-0.56, indicating the ISO method was reporting higher values of turbidity in the lower range (i.e., 0-5 NTU). Results of the single fit regressions between each mode of ISO measurements and EPA Field measurements are visualized below in Figure 7. Furthermore, unlike in the full range, temperature did not exhibit significant effects on the prediction of EPA Field values from ISO values. Interestingly, the closest to 1:1 relationship between any EPA and ISO measurement set collected in this study was found in the sensitized grouping analysis; the coefficients of EPA Field and ISO Delay models varied between 0.96 and 1.09, indicating approximately equivalent predictions of turbidity (Table 11). Surprisingly, the 1:1 relationship between EPA Field and ISO Delay measurements in the sensitized grouping analysis became more similar; this contradicts the relationships of EPA Field versus immediate ISO analyses (In Situ or Field) in which ISO measurement comparisons became more dissimilar (overestimating) in the sensitized analysis. Finally, water color helped the prediction of EPA Field measurements from ISO Delay measurements, by correcting with a negative coefficient (negative EPA bias), similar to EPA Delay predictions when using ISO Delay (Table 11).

Table 11. As for Table 9, multilinear regression models are presented which assess comparability between EPA Field turbidity values (response) to different ISO turbidity values (predictor) collected at different locations/times; data in these models were restricted by the condition EPA Field < 5 NTU. $p < 0.05$: *; $p < 0.01$: **; $p < 0.001$: ***; $p < 0.0001$: ****.

Condition: EPA Field <5 NTU	Response: EPA Field				
Independent Variables	Coefficient	Coefficient2	p	p2	R^2
ISO In Situ	0.528		***		0.773
ISO In Situ + Salinity	0.527	-0.002	***		0.768
ISO In Situ + In Situ Temperature	0.512	-0.132	***		0.772
ISO In Situ + Color 412	0.526	-0.007	***		0.688
ISO Field	0.550		***		0.783
ISO Field + Salinity	0.546	0.005	***		0.779
ISO Field + Field Temperature	0.558	0.064	***		0.780
ISO Field + Color 412	0.525	-0.003	***		0.765
ISO Delay	1.09		***		0.715
ISO Delay + Salinity	1.08	0.009	***		0.712
ISO Delay + Delay Temperature	1.07	0.162	***		0.723
ISO Delay + Color 412	0.963	-0.043	***	*	0.751

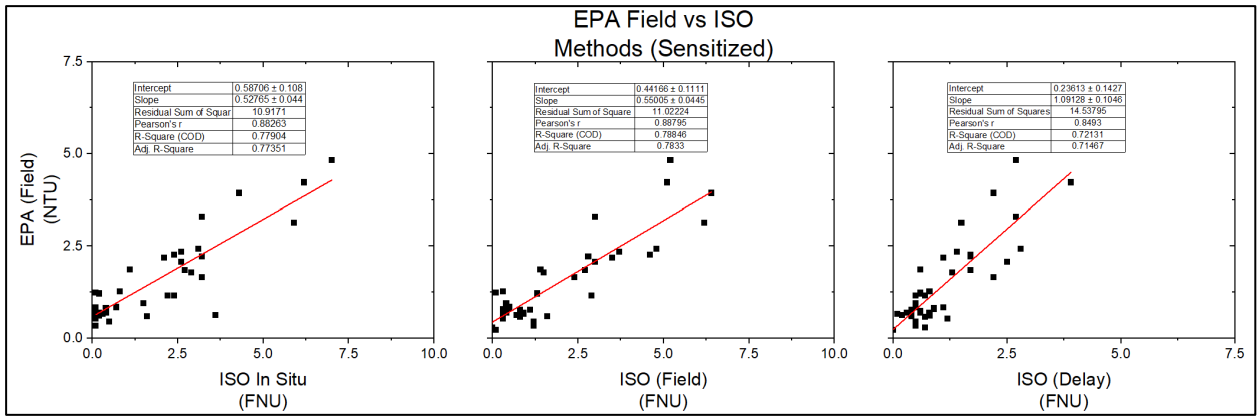

Figure 7. Covariates are visualized comparing the EPA values collected in the field with the three ISO measurement locations, while data for the models was restricted by the condition EPA Field < 5 NTU, as for Table 11.

Finally, predictive models for the EPA Delay measurements were constructed from the same parameters as Table 11 and 12. Fits of the EPA Delay vs ISO Field measurements degenerated the most (R^2 = 0.59-0.70; Table 12 & Figure 8) in the sensitized analysis compared to the full range of turbidities (i.e. in comparison to Table 10). Also, similar to the trend from the sensitized models predicting EPA Field (Table 11), the decrease in goodness of fit was accompanied by increasing overestimation of EPA Delay turbidity for both immediate ISO analyses (In Situ & Field, coefficients: 0.36-0.42). Overall, these findings are in good agreement that results of significant difference are only observed during location-based pairing (i.e. Delay vs. In Situ or Field) in the sensitized dataset (See "Overview of Method Comparability", Table 6). Again temperature, but not salinity, showed a significant effect on the estimation of the EPA Delay measurements with respect to the ISO In Situ measurements (Table 12). However, the temperature coefficient is assumed to negatively bias the ISO method because water absorption increases as a function of temperature primarily in the NIR band range (Sullivan et al., 2006) used by the ISO method sensors. Therefore, by increasing absorption, the amount of scattered light which is detected by the instrument will decrease. Nevertheless, the temperature coefficient was found to be negative (coefficient = -0.37735) indicating that temperature positively biased ISO measurements in the EPA Delay vs ISO In Situ sensitized model. Again, the negative bias of water color on the EPA method was illustrated in this set of analyses by showing significant effects of water color on the prediction of EPA Delay measures from ISO Delay measures (Table 12).

Table 12. As for Table 10, multilinear regression models are presented which assess comparability between EPA Delay turbidity values (response) with ISO turbidity values (predictor) collected at different locations/times; data in these models were restricted by the condition EPA field < 5 NTU. p < 0.05: *; p < 0.01: **; p < 0.001: ***; p < 0.0001: ****.

Condition: EPA Field <5 NTU	Response: EPA Delay				
Independent Variables	Coefficient	Coefficient2	p	p2	R^2
ISO In Situ	0.380		***		0.657
ISO In Situ + Salinity	0.408	0.118	***		0.660
ISO In Situ + In Situ Temperature	0.377	-0.377	***	**	0.707
ISO In Situ + Color 412	0.423	0.005	***		0.628
ISO Field	0.373		***		0.602
ISO Field + Salinity	0.374	-0.001	***		0.593
ISO Field + Field Temperature	0.360	-0.108	***		0.601
ISO Field + Color 412	0.390	0.005	***		0.618
ISO Delay	0.937		***		0.884
ISO Delay + Salinity	0.951	0.039	***		0.885
ISO Delay + Delay Temp	0.921	0.091	***		0.885
ISO Delay + Color 412	0.866	-0.024	***	*	0.906

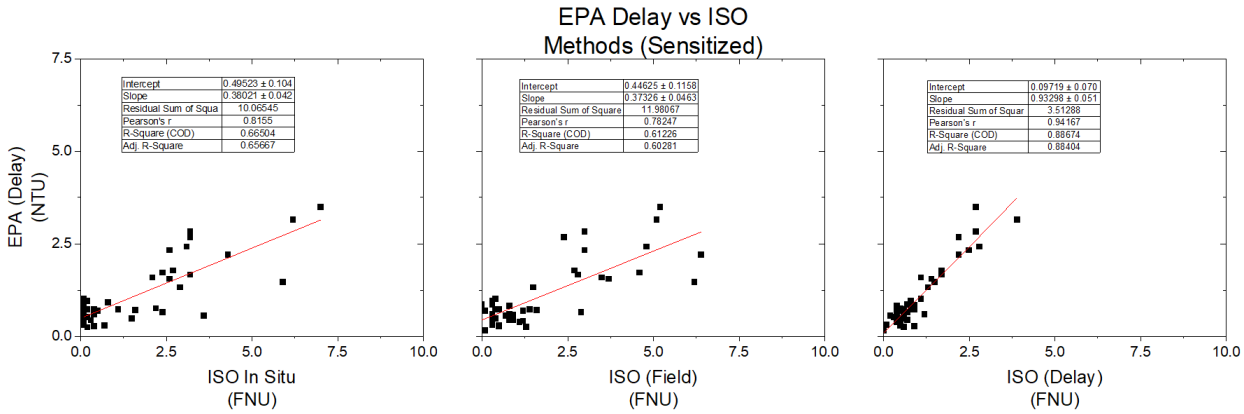

Figure 8. Covariates are visualized comparing the EPA Delay values with the three ISO measurement locations, while data for the models was restricted by the condition EPA Field < 5 NTU (as for Table 12).

In summary, this set of analyses illustrates that the EPA method is comparable to the ISO method over wider ranges of turbidity (0-30 NTU) indicated by $R^2 > 0.9$ and coefficients which vary within a small range. A number of comparisons are made, some which may be more applicable in practice than others. Restricting the interpretation of results to comparisons of ISO versus EPA solely within either immediate *or* delayed modes always resulted in better fits than when comparing delayed versus immediate measurement sets (Table 9-12). For example, the range of R^2 in the full-range EPA Delay models (Table 10) was 0.98-0.99 in mixed models that incorporated the ISO Delay analyses, compared to a range of 0.91-0.94 for mixed models that

instead used immediate ISO measurements (In Situ or Field). Temperature and salinity both affect IOPs in the spectral range specific to the ISO method. While salinity had no significant effects in any of the mixed models, temperature affected all ISO measurement predictions of EPA Field turbidity in the full range analysis (Table 9) but not for the same EPA Delay models (Table 10). In contrast, temperature did not affect any ISO predictions of EPA Field measurement in the sensitized analysis (Table 11) and affected the prediction of EPA Delay measurements only when the ISO In Situ measurements were used (Table 12). The contrasting trends of temperature effects are further complicated by the coefficients which had opposite signs (effects) on the predictions of EPA measurements between full range EPA field models (Table 10) and the sensitized EPA delayed models (Table 12).

Finally, although sensitized models (turbidity range of 0-5 NTU) generally performed worse than full range models, this was not as drastic in sensitized models predicting EPA Delay measures from ISO Delay measures (Table 12). First, when switching from EPA Field predictions made by immediate ISO (Field and In Situ) measurements in full range models to the sensitized models, the range of the coefficients decreased from 0.78-0.82 to 0.52-0.55; this was accompanied by decreases in the goodness of fit: R^2 from 0.95-0.96 to 0.68-0.78 (Tables 11 and 12). The concurrent decreases in both coefficients and R^2 between similar models which are separated only by the range of turbidity (sensitivity) reflects that there may be more uncertainty in predicting exact comparisons between the EPA and ISO methods at lower turbidities. However, the range of coefficients was comparable in EPA Delay predictions from ISO Delay measurements between the full range models (coefficients: 0.85-0.90) and sensitized models (coefficients: 0.86-0.95); also, the goodness of fit from the full range model (R^2: 0.98-0.99) decreased in the sensitized model (R^2: 0.88-0.90). Therefore, the comparison of delayed ISO and EPA measurements may be comparable between sensitized and full range turbidity models because coefficients from the sensitized model have larger errors that incorporate the coefficients produced by full range models.

Prediction of TSS From Turbidity

Turbidity is a parameter often used as a predictor of SPM which is typically derived from direct methods like TSS. This is particularly desirable information when monitoring impacts due to activities causing sediment resuspension, such as dredging. Therefore, turbidity and TSS, as predictors of SPM, should exhibit some degree of covariance. Analysis of covariance (ANCOVA) models were built with TSS implemented as the response variable. In the ANCOVAs, the turbidity analytical method and location were used as grouping variables, for independently measured turbidity values (e.g., EPA Field). The analytical method grouping splits measurements of turbidity into three broad classes (EPA, ISO, and In Situ) to predict TSS from turbidity measurements within those groupings. The location grouping splits measurements of turbidity into three other groups (Field, Delay, and In Situ; Table 4) to predict TSS from turbidity within those groupings. The two constructed ANCOVA's ultimately reveal that TSS and turbidity do not significantly covary (neither linear nor exponential) and there is no effect of the grouping variables on predictions of TSS from turbidity (Table 13).

Table 13. Results of the analysis of covariance which sought to predict TSS within groups of method/location using turbidity as a covariate. There is no significant relationship between TSS and turbidity within method/location groups demonstrated by p values > 0.05, and the calculated F-stat is shown for model transparency.

ANCOVA		Results	
Formula	Independent/Covariate	F-stat	p-value
TSS~Method + Turbidity	Method (ISO, EPA, in situ)	0.054	0.995
	Turbidity	2.258	0.138
TSS~Location +Turbidity	Location (Field, Delay, ISO In Situ)	0.109	0.897
	Turbidity	2.62	0.134

Next, multilinear regression models were constructed to verify whether accounting for interferences in the turbidity method could resolve its relationship with TSS. Models predicting TSS were additively constructed using turbidity and an increasing number of potential turbidity measurement interferences (salinity, temperature, water color, dFe, and DOC). The first constructed model was a single linear regression model which fit the relationship between TSS and turbidity (Table 14); this showed an unexplainable negative correlation between TSS and turbidity, was not significant ($p > 0.05$), and was poorly fit ($R^2 = 0.004$). Furthermore, adding interferences did not improve fits toward something which could plausibly be developed into a correction method that can predict TSS using turbidity. For example, the maximally parameterized model showed significant effects between predictors (turbidity + interferences) and the response variable (TSS), however the overall fit was still relatively poor ($R^2 = 0.21$). Analysis of the residuals further revealed that significant effects were mostly due to weighting errors in the model caused by outliers (not shown). Importantly, data manipulation (e.g., transformation, outlier removal) was carefully avoided in presented model summaries (Table 14) to simulate real-world encountered environmental sampling. Fortunately, most departures from normality are caused by drastic differences in parameters like salinity, dFe, and DOC between the estuary and ECA. Therefore, the following bounds were implemented to restrict the dataset: salinity>34.59 PSU and dFe < 0.06 μM (Fe serves as a tracer for terrestrial/marine mixing); this restriction on the acceptable model values effectively reduced the number of samples from 63 to 42, helped avoid the need to eliminate outliers, and made the dataset more normal overall. Reapplying the all-parameter model (TSS~Turbidity+Salinity+Temp.+Color+dFe+DOC) to the normalized dataset further showed the effect of outliers on the original model fit, reducing the R^2 from 0.2121 to 0.02841 and removing the significance of all parameters except dFe (dFe, p=0.01; not tabulated).

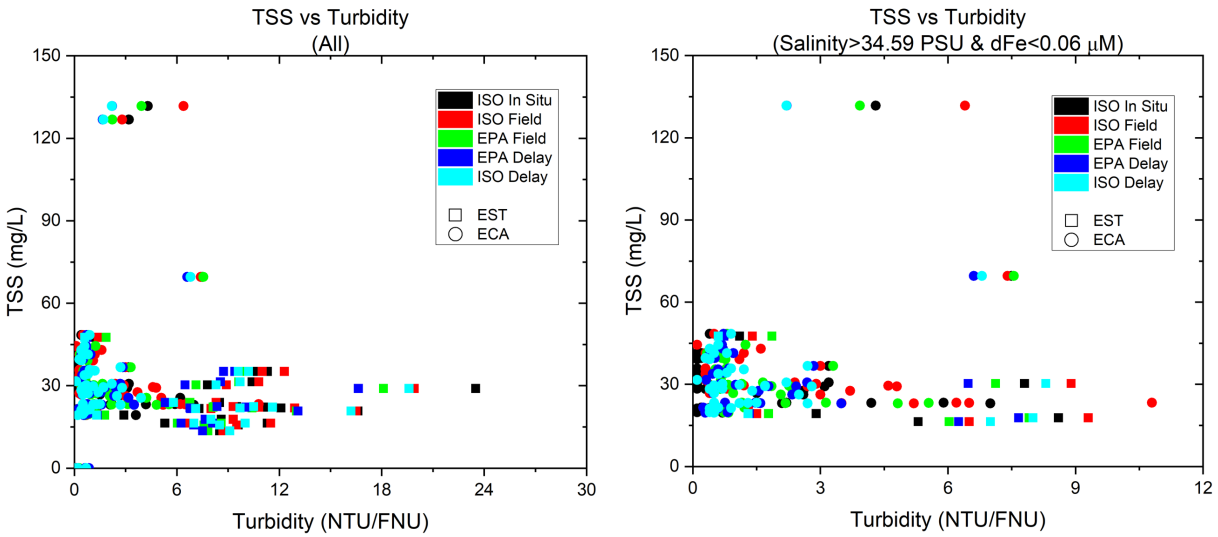

Figure 9. Insignificance in the covariance between TSS and turbidity is further demonstrated in the non-descriptive correlation. All values are colored acccording to the five measurement techniques (i.e., EPA Field/Delay, ISO Field/Delay, and ISO In Situ) and further specified by shape for estuarine (square) and ECA (circle) sites. All turbidity values are presented for comparison (left) as well as an additional condition based visualization that represents only marine sites (right).

Table 14. Results of additively constructed multilinear regressions attempting to predict TSS from turbidity suggest that TSS cannot be estimated from turbidity or ancillary data, supported by a maximum R^2 of 0.2152. Importantly, ancillary data was non-normal, leading to pseudo-significant effects of some predictors (e.g., salinity, DOC, dFe). While data normalization techniques were avoided, a full account of the results (R^2+p-value) emphasize the non-normality. Models in which normalized data returned much lower R^2 and no significance are not tabulated. $p < 0.05$: *; $p < .01$: **; $p < 0.001$: ***; $p < 0.0001$: ****.

	Response: TSS												
Independent Variables	Turbidity (T)	Salinity (S)	Temp. (Te)	Color 412 (C)	dFe (F)	DOC (D)	p	p2	p3	p4	p5	p6	r2
T	-0.405	-	-	-	-	-							0.004
T+S	0.655	0.8963		-	-	-	*	***					0.1199
T+S+Te	0.66334	0.89917	-0.07016	-	-	-	*	***					0.1113
T+S+Te+C	1.03512	0.82635	-0.08926	-0.28743	-	-	*	***					0.126
T+S+Te+C+F	0.43997	0.93501	0.06539	-0.6318	249.42655	-		***		**	***		0.2152
T+S+Te+C+F+D	0.547892	0.924984	0.050148	-0.572824	269.7739	-0.007311		***		*	***		0.2121

Recommendations

In conclusion, this study has found that EPA 180.1 and ISO 7027 sensors are highly comparable over a wide range of turbidity values indicated by linear fits which returned R^2 values > 0.9 between 0-30 NTU/FNU. Furthermore, pairwise-t-tests and one-way ANOVAs both demonstrated similar findings by comparing turbidity values within ISO 7027 and EPA 180.1 groups, also returning no significant differences between groupings. Furthermore, EPA 180.1 and ISO 7027 were most often best correlated when the two methods were compared between similar analysis location; for example, EPA 180.1 field turbidity values are most comparable with ISO 7027 field samples as opposed to EPA 180.1 field versus in situ (ISO 7027) or delayed ISO 7027 samples. Nevertheless, comparisons between ISO in situ and EPA 180.1 turbidity values never suggested that the two were significantly different. Therefore, it is possible that the ISO 7027 method can be used in place of EPA 180.1 method in estuarine and coastal waters with less than 30 NTU/FNU (at least using our selected sensor, the Hanna Instruments HI9829) given that the two are generally in agreement with each other. Caution should be warranted, however, as some significant sensitivity deviations between even ISO 7027 compliant probes have been reported for standardized particle solutions (Davies-Colley et al. 2021). We therefore recommend consistent use of a single manufacturer's ISO 7027 sensor, or that regional calibrations be conducted to allow standardization of ISO-collected data to conform with a collection of EPA 180.1 data.

While the relative responses for a set of samples (e.g., a continuous time-series trend) should behave as expected, the deviation from a 1:1 response does suggest an opportunity for ISO 7027 measurement empirical correction to conform to an existing EPA 180.1 database. The realized coefficients between ISO 7027 and EPA 180.1-configured sensor measurements were typically within the range of (m = 0.77-0.85 where ISO = m * EPA), suggesting higher turbidity measurements by the ISO 7027 method relative to the DEP SOP-approved EPA 180.1 method. Temperature and water color both showed significant effects in multilinear regressions between the ISO 7027 and EPA 180.1 recorded turbidity values. Temperature may exert a negative bias (i.e., lower turbidity) on the ISO 7027 method because of temperature dependent absorption peaks in the band-range of the ISO 7027 sensor; however, its coefficient shows an inconsistent sign (i.e., positive or negative) meaning modeled effects of temperature suggest both positive and negative biases on the ISO turbidity measurement, contrary to theory. Also, temperature never significantly improved model fit suggesting very minor effects of temperature on turbidity detection between methods. On the other hand, water color consistently suggested a negative bias on the EPA 180.1 method (i.e., lower sensitivity of turbidity by EPA 180.1 sensor in the presence of color) through an always negative coefficient (e.g., Figure 10). It is unclear why color was so significant in the prediction of EPA 180.1 turbidity measurements (delayed) specifically from the ISO 7027 delayed method. Coefficients typically decreased for ISO Delay measurements relative to immediate EPA Field (methods more dissimilar) which may emphasize the color effect; however, time dependent effects such as precipitation of colored particulates may make the methods more dissimilar over time. Nevertheless, this negative bias by color may explain larger turbidity measurements by the ISO 7027 method. For a complete understanding of color effects, a secondary study may need to be conducted with more sites in the EST, because some color data was not reported due to method detection limits within the ECA.

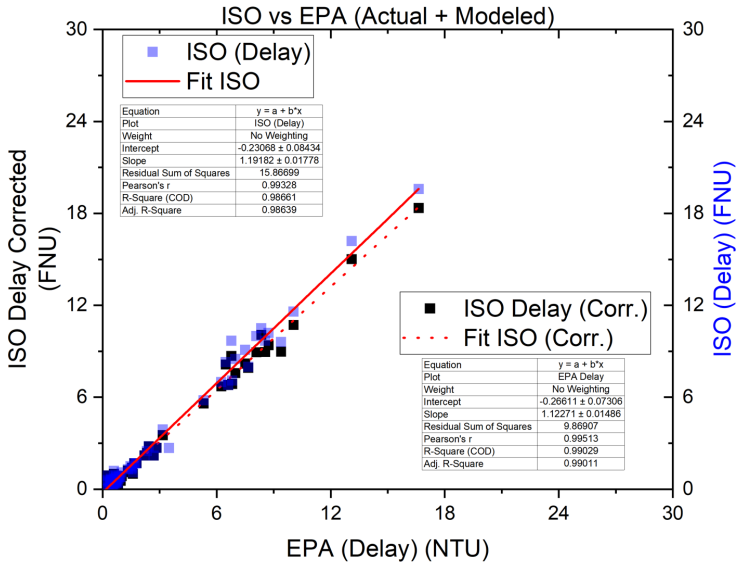

Figure 10. Modeling ISO values using the most significant water color coefficient from Table 10. The decrease in the slope when accounting for water color brings the slope closer to a value of 1 (i.e., Slope=1 means equal measurements between methods) and slightly improved the R^2 (0.986->0.990).

In addition, ISO 7027 and EPA 180.1 methods were still comparable even in sensitized models where turbidity was limited to an EPA turbidity value < 5 NTU. The overall R^2 decreased from a range of 0.95-0.96 for the full dataset to 0.77-0.88 in the sensitized datasets between similar analysis locations (i.e., for models of EPA Field vs ISO Field/ISO In Situ, or EPA Delay vs ISO 7027 Delay). Nevertheless, it was shown that for SLE site SLE-ME, discrete samples from the current study do not capture the full range of turbidities found when compared to the continuous in situ data provided by the Indian River Lagoon Observatory Network (Figure 3). There is an overall good fit ($R^2 > 0.77$) between the established EPA 180.1 method and the tested ISO 7027 methods under high and low turbidity conditions and reproducible coefficients over the larger turbidity range (0.77-0.85; turbidity: 0-30 NTU/FNU). Coefficients of EPA Field vs ISO In Situ turbidity measurement (Table 9 and 11) were then used to generate a protocol for converting between EPA and ISO 7027 In Situ measurements depending on recorded turbidities (Figure 11). The generated equations were then used to estimate corrected ISO 7027 turbidities, which are plotted versus the true EPA 180.1 measurements (Figure 12). The created models show that the high turbidity correction slightly improved the fit and, more importantly, changed the slope from 1.22 to 0.96. The modeled slope decreased the agreement error (i.e., difference from the slope of 1) from 22% to 4% between the two methods. The low turbidity model brought agreement error from 41% to 22%; the agreement error is at least in part due to the lesser R^2 under low turbidity conditions and the lack of corrective terms (e.g., temperature). Continuous, in situ deployments of ISO 7027 sensors will also have an added benefit of data continuity, essentially producing more data over time that can be used to continuously improve correction algorithms to generate a corresponding EPA turbidity.

Finally, TSS showed a poor fit with turbidity in the mixed SLE/ECA dataset (Table 14) and marine specific data set (Figure 9). The poor fit is likely due to the natural variability of size

and composition of attenuating particles in the environment (Boss et al., 2009). The importance of solid-phase influences on the TSS prediction from turbidity is emphasized by multilinear regressions which incorporated dissolved parameters that interfere with turbidity measurements (e.g., color, temperature, salinity), but could not help the prediction. Thus, if true measurements of suspended sediments are desired for environments such as the ECA, alternative methods should be pursued.

Overall, this project is a continued effort to improve turbidity monitoring practices and our understanding of background turbidity in the ECA (and throughout Florida's Coral Reefs). We recommend that DEP incorporate continuous ISO 7027 turbidity monitoring technology used regularly in scientific research and industry into its SOPs; however, a site-specific – and perhaps an ISO 7027 sensor manufacturer-specific empirical correction scheme should be employed to ensure best compatibility with existing EPA 180.1 data. Furthermore, this project lays the groundwork for incorporating historical and new ISO 7027 instrument data into WIN, overall increasing our understanding of background turbidity in the ECA. Finally, data collected during this project and historical projects in which turbidity was monitored could supplement DEP's Division of Environmental Assessment and Restoration's (DEAR) triennial review process and overall, the modification of the turbidity criterion (FAC 62-302).

As far as next steps, we recommend exploring the deviations of turbidity from TSS, and determining how best to definitively measure suspended sediment concentrations in situ. For example, dredging activities must remain under a specific turbidity threshold relative to background levels. As TSS was not able to measure turbidity (anticorrelated in fact), then turbidity would be a poor metric for understanding particulate suspension and deposition, e.g., as it affects coral reefs. More advanced – albeit more expensive – sensors are commercially available that are capable of monitoring particle density and particle size distribution, such as the Sequoia Scientific LISST. While sustained and widespread employment of these sensors may exceed DEP's budget constraints, a discrete, multisensor, co-deployment effort seeking to unravel how TSS, particle size/density, and turbidity (i.e. ISO 7027) are related could enable an improved understanding of how, if at all, turbidity represents some measure of TSS. Simultaneously, bottom-mounted underwater multispectral light sensors could simultaneously reveal how underwater light transmission – in particular those wavelengths that affect coral health – behaves as a function of particle size distribution. Ultimately, the results of this proposed effort could prescribe appropriate monitoring programs mandated during dredging and restoration activities, as well as the redefining of acceptable turbidity and/or suspended sediment concentrations incurred during these activities.

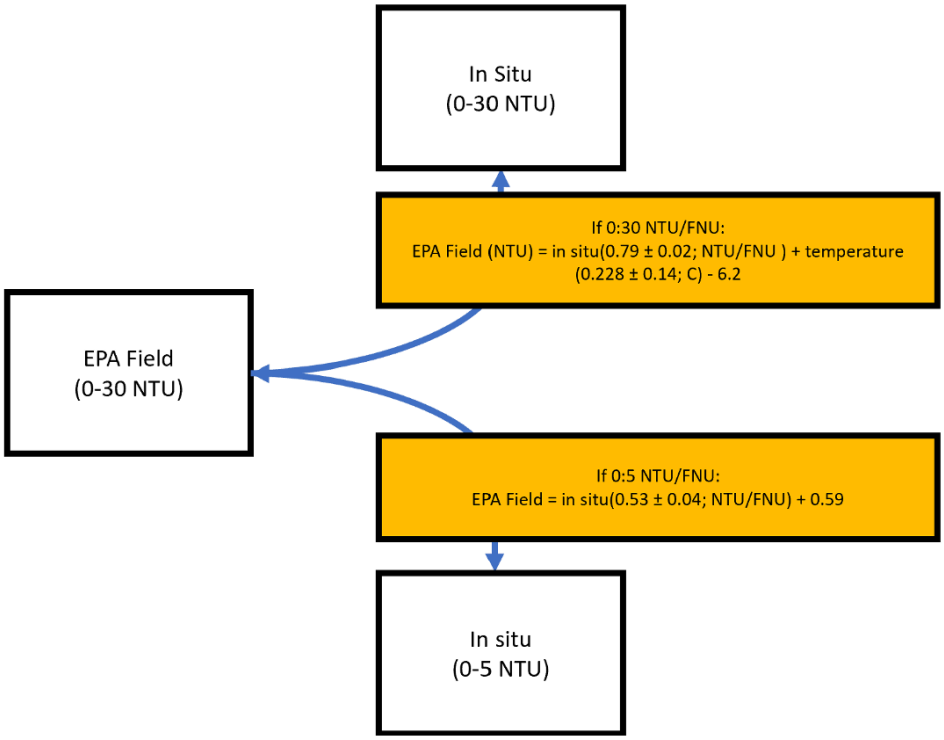

Figure 11. Procedure for correcting ISO 7027 measurements to yield equivalent EPA 180.1 values. Correction equations are presented under high and low turbidity conditions using coefficients from Tables 9 and 11, along with associated standard errors, and model intercepts.

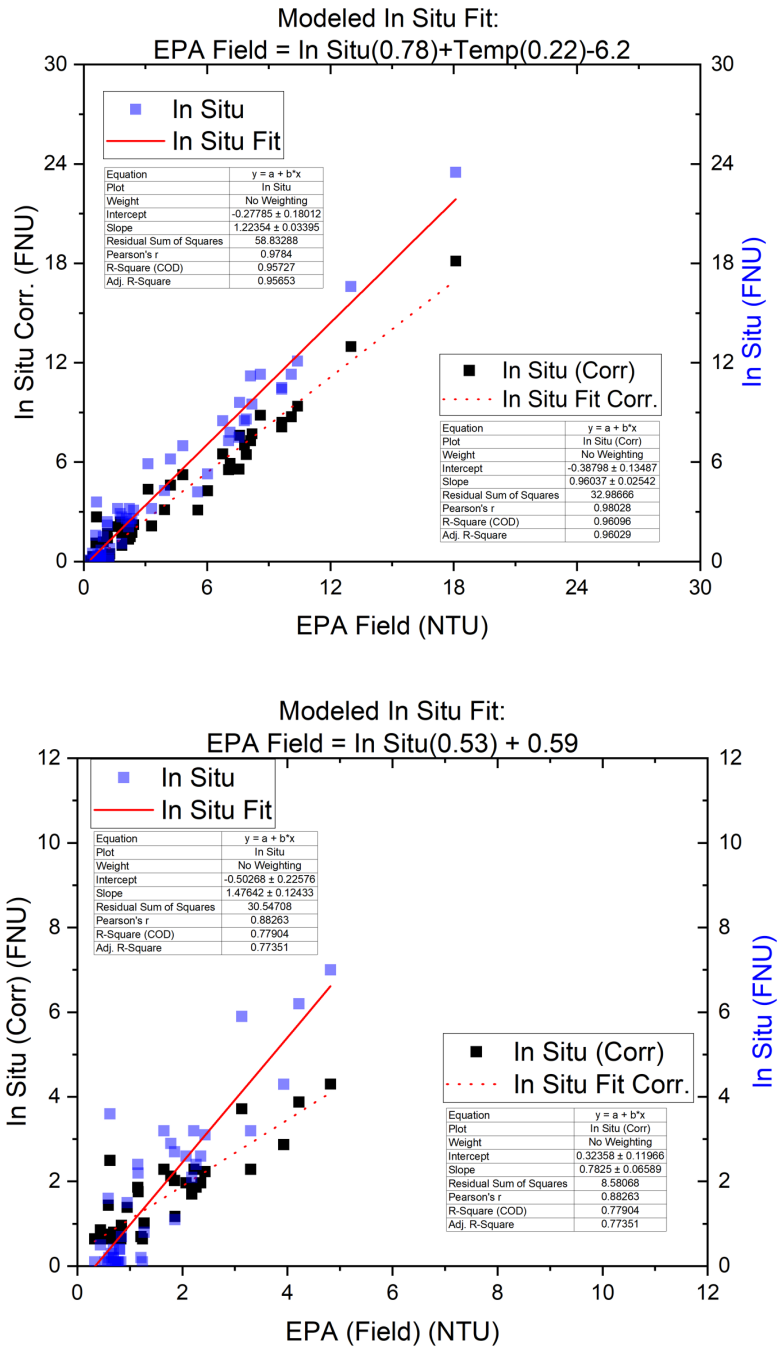

Figure 12. Results of applications of the Figure 10 empirical correction procedure and equations to use in situ ISO 7027 values from a high (top) and low turbidity datasets (bottom).

References

Florida Department of Environmental Protection. (2017). FT 1600: Field Measurement of Turbidity. https://www.flrules.org/gateway/readRefFile.asp?refId=7972&filename=FT%201600_Jan2017.docx.

Boss, E., Slade, W., & Hill, P. (2009). Effect of particulate aggregation in aquatic environments on the beam attenuation and its utility as a proxy for particulate mass. *Optics express*, *17*(11), 9408-942

Davies-Colley, R., Hughes, A. O., Vincent, A. G., & Heubeck, S. (2021). Weak numerical comparability of ISO-7027-compliant nephelometers. Ramifications for turbidity measurement applications. *Hydrological Processes*, *35*(12), e14399.

International Organization for Standardization. (2016). Water quality — Determination of turbidity — Part 1: Quantitative methods.

Kirk, J. T. (1994). Light and photosynthesis in aquatic ecosystems. Cambridge university press.

Logozzo, L.A., Martin, J.W., McArthur, J. et al. (2022). Contributions of Fe(III) to UV–Vis absorbance in river water: a case study on the Connecticut River and argument for the systematic tandem measurement of Fe(III) and CDOM. Biogeochemistry 160, 17–33. https://doi.org/10.1007/s10533-022-00937-5.

Sadar, M. (2004). Making sense of turbidity measurements – Advantages in establishing traceability between measurements and technology. 4th National Monitoring Conference, Chattanooga, Tennessee May 17-20. https://acwi.gov/monitoring/conference/2004/conference_agenda_links/papers/poster_papers/215_SadarMike.pdf.

Sullivan, J. M., Twardowski, M. S., Zaneveld, J. R. V., Moore, C. M., Barnard, A. H., Donaghay, P. L., & Rhoades, B. (2006). Hyperspectral temperature and salt dependencies of absorption by water and heavy water in the 400-750 nm spectral range. Applied Optics, 45(21), 5294-5309.

U.S. Environmental Protection Agency. (1993). Method 180.1: Determination of Turbidity by Nephelometry.

American Public Health Association, American Water Works Association, Water Environment Federation. Lipps WC, Braun-Howland EB, Baxter TE, eds. (2013) *Standard Methods for the Examination of Water and Wastewater*. 24th ed. Washington DC: APHA Press.

Xiao, Yi-Hua, Sara-Aho, Timo, Hartikainen, Helinä, Vähätalo, Anssi V. (2023). Contribution of ferric iron to light absorption by chromophoric dissolved organic matter, Limnology and Oceanography 58, doi: 10.4319/lo.2013.58.2.0653.

Appendix 1: Raw Sample Metadata

ID	Site	Date	Time	Depth	Latitude	Longitude	Survey
230901	SLE-SF	4/22/23	14:25	Surface	27.18919	-80.2646	1
230902	SLE-SF	4/22/23	-14:34	0.5 m	27.18919	-80.2646	1
230903	SLE-ME	4/22/23	13:58	Surface	27.20746	-80.2509	1
230904	SLE-ME	4/22/23	14:09	2.4 m	27.20746	-80.2509	1
230905	SLE-IN	4/22/23	13:22	Surface	27.1634	-80.1725	1
230906	SLE-IN	4/22/23	13:34	4.9 m	27.1634	-80.1725	1
230907	ECA-T1	4/22/23	12:58	Surface	27.16052	-80.1452	1
230908	ECA-T1	4/22/23	13:06	4.4 m	27.16052	-80.1452	1
230909	ECA-T2	4/22/23	12:34	Surface	27.16135	-80.1374	1
230910	ECA-T2	4/22/23	12:47	9.3 m	27.16135	-80.1374	1
230911	ECA-T3	4/22/23	12:11	Surface	27.16277	-80.1266	1
230912	ECA-T3	4/22/23	12:23	13.7 m	27.16277	-80.1266	1
230913	ECA-T4	4/22/23	11:48	Surface	27.14995	-80.1324	1
230914	ECA-T4	4/22/23	11:59	9.4 m	27.14995	-80.1324	1
230915	ECA-T5	4/22/23	11:27	Surface	27.14191	-80.1393	1
230916	ECA-T5	4/22/23	11:36	Bottom (depth not record)	27.14191	-80.1393	1
230917	ECA-T6	4/22/23	11:05	Surface	27.14155	-80.1286	1
230918	ECA-T6	4/22/23	11:16	10.2 m	27.1415 d5	-80.1286	1
230919	ECA-T7	4/22/23	10:28	Surface	27.14331	-80.1186	1
230920	ECA-T7	4/22/23	10:47	13.2 m	27.14331	-80.1186	1
230921	Deionized water	4/22/23	10:17	Blank	27.18919	-80.2646	1
231701	SLE-ME2	5/10/23	11:43	Surface	27.19308	-80.2056	2
231702	SLE-ME2	5/10/23	11:51	2 m	27.19308	-80.2056	2
231703	SLE-ME	5/10/23	11:14	Surface	27.20752	-80.2508	2
231704	SLE-ME	5/10/23	11:27	2 m	27.20752	-80.2508	2
231705	SLE-IN	5/10/23	10:48	Surface	27.1636	-80.173	2
231706	SLE-IN	5/10/23	10:55	3 m	27.1636	-80.173	2
231707	ECA-T1	5/10/23	9:42	Surface	27.16002	-80.1444	2
231708	ECA-T1	5/10/23	9:49	3 m	27.16002	-80.1444	2
231709	ECA-T2	5/10/23	9:27	Surface	27.16081	-80.1359	2
231710	ECA-T2	5/10/23	9:32	9 m	27.16081	-80.1359	2

231711	ECA-T3	5/10/23	9:07	Surface	27.1645	-80.1253	2
231712	ECA-T3	5/10/23	9:15	13 m	27.1645	-80.1253	2
231713	ECA-T4	5/10/23	8:44	Surface	27.1508	-80.1326	2
231714	ECA-T4	5/10/23	8:52	7 m	27.1508	-80.1326	2
231715	ECA-T5	5/10/23	8:13	Surface	27.14179	-80.137	2
231716	ECA-T5	5/10/23	8:16	3 m	27.14179	-80.137	2
231717	ECA-T6	5/10/23	10:05	Surface	27.14242	-80.128	2
231718	ECA-T6	5/10/23	10:12	9 m	27.14242	-80.128	2
231719	ECA-T7	5/10/23	10:22	Surface	27.14337	-80.119	2
231720	ECA-T7	5/10/23	10:24	13 m	27.14337	-80.119	2
231721	Deionized water	5/10/23	N/A	Blank	27.14337	-80.119	2
231801	SLE-ME2	5/11/23	16:11	Surface	27.19108	-80.2051	3
231802	SLE-ME2	5/11/23	16:22	Bottom (depth not recorded)	27.19108	-80.2051	3
231803	SLE-ME	5/11/23	15:53	Surface	27.20772	-80.2508	3
231804	SLE-ME	5/11/23	15:59	2.2 m	27.20772	-80.2508	3
231805	SLE-IN	5/11/23	15:27	Surface	27.16362	-80.1731	3
231806	SLE-IN	5/11/23	15:36	5.7 m	27.16362	-80.1731	3
231807	ECA-T1	5/11/23	15:03	Surface	27.16052	-80.1454	3
231808	ECA-T1	5/11/23	15:15	3.1 m	27.16052	-80.1454	3
231809	ECA-T2	5/11/23	14:28	Surface	27.16096	-80.1367	3
231810	ECA-T2	5/11/23	14:50	9.8 m	27.16096	-80.1367	3
231811	ECA-T3	5/11/23	14:11	Surface	27.16321	-80.1263	3
231812	ECA-T3	5/11/23	14:19	13.7 m	27.16321	-80.1263	3
231813	ECA-T4	5/11/23	13:32	Surface	27.15013	-80.133	3
231814	ECA-T4	5/11/23	13:42	9.6 m	27.15013	-80.133	3
231815	ECA-T5	5/11/23	13:17	Surface	27.14118	-80.1375	3
231816	ECA-T5	5/11/23	13:25	2.5 m	27.14118	-80.1375	3
231817	ECA-T6	5/11/23	13:00	Surface	27.14187	-80.1277	3
231818	ECA-T6	5/11/23	13:10	10.6 m	27.14187	-80.1277	3
231819	ECA-T7	5/11/23	12:43	Surface	27.14255	-80.1191	3
231820	ECA-T7	5/11/23	12:53	12.7 m	27.14255	-80.1191	3
231821	Deionized water	5/11/23	11:51	Blank	27.14337	-80.119	3

Appendix 2: Raw Sample Data

ID	Salinity (PSU)	ISO In Situ (FNU)	ISO Field (FNU)	EPA Field (NTU)	ISO Delay (FNU)	EPA Delay (NTU)	TSS (mg/L)	CU456 (CU)	CU412 (CU)	DOC (uM)	TN (uM)	dFe (uM)	In Situ Temp (C)	Field Temp (C)	Delay Temp (C)
230901	11.19	16.6	16.5	13.00	16.2	13.10	20.8	31.5	38.4	nm	nm	0.155	27.22	27.78	20.34
230902	14.07	23.5	19.9	18.10	19.6	16.63	29.0	33.0	40.5	778.5	32.30	0.132	26.33	26.83	22.63
230903	16.77	9.6	9.5	7.59	8.5	6.99	15.7	24.5	29.9	476.3	23.77	0.074	27.91	28.24	22.99
230904	17.25	11.3	11.5	8.59	10.0	8.09	16.4	27.9	34.3	522.0	20.75	0.075	27.40	27.76	22.64
230905	36.06	7.8	8.9	7.12	8.3	6.48	30.3	4.0	5.4	135.1	10.47	0.015	26.21	26.93	22.49
230906	36.13	8.6	9.3	7.91	8.0	7.66	17.8	BDL	2.5	118.2	8.47	0.011	26.11	26.54	22.89
230907	36.58	4.3	6.4	3.93	2.2	2.21	131.7	BDL	BDL	122.8	6.84	0.034	26.34	26.65	22.65
230908	36.48	7.5	7.4	7.55	6.8	6.61	69.6	BDL	BDL	82.4	5.38	0.008	26.24	26.45	24.35
230909	37.21	2.6	3.0	2.07	2.5	2.34	26.3	6.0	4.1	126.5	8.19	0.031	25.96	25.50	22.65
230910	37.87	2.7	2.7	1.85	1.7	1.78	29.3	2.6	BDL	90.5	6.63	0.013	25.72	25.90	22.58
230911	37.48	0.8	0.3	1.27	0.8	0.92	27.2	BDL	BDL	98.4	5.40	0.117	26.34	26.97	22.53
230912	38.01	2.1	3.5	2.18	1.1	1.59	23.1	5.5	3.0	150.1	13.42	0.011	25.70	26.39	22.55
230913	37.03	2.6	3.7	2.35	1.4	1.55	27.6	3.6	BDL	75.4	5.62	0.009	26.05	26.47	22.28
230914	37.78	3.2	2.4	1.65	2.2	2.69	30.7	BDL	BDL	75.9	6.33	0.024	25.75	25.93	22.39
230915	35.57	3.1	4.8	2.43	2.8	2.43	29.2	BDL	BDL	151.4	8.43	0.023	26.28	26.81	22.33
230916	37.68	2.4	4.6	2.26	1.7	1.73	29.5	BDL	BDL	129.9	9.05	0.012	25.79	26.03	22.47
230917	37.12	3.2	2.8	2.22	1.7	1.67	126.8	BDL	BDL	98.7	6.81	0.102	25.84	26.66	22.44
230918	37.90	2.2	10.8	1.16	0.5	0.76	23.3	BDL	BDL	64.3	4.04	0.002	25.38	26.25	23.94
230919	38.02	0.3	0.9	0.65	0.4	0.43	28.3	BDL	BDL	85.1	4.27	0.009	26.20	26.32	23.77
230920	38.66	3.2	3.0	3.30	2.7	2.84	36.7	2.5	BDL	68.1	4.17	0.002	25.28	26.13	24.00
230921	0.01	nm	0.1	0.22	0.0	0.16	BDL	0.0	BDL	34.0	3.00	0.012	nm	24.05	23.65

231701	21.71	10.4	10.8	9.63	9.7	8.55	31.4	18.9	24.3	312.7	20.83	0.074	24.05	27.72	21.88
231702	24.08	11.3	12.3	10.10	9.6	9.39	35.2	15.9	20.2	311.8	20.37	0.063	27.36	27.34	21.82
231703	14.10	11.2	10.8	8.12	11.6	10.05	22.2	22.5	28.4	479.7	26.93	0.133	27.13	21.26	21.93
231704	17.86	12.1	12.9	10.40	9.7	6.77	21.9	26.4	32.3	388.3	24.39	0.042	27.93	27.40	23.09
231705	34.20	7.3	8.0	7.05	7.1	6.81	21.7	6.5	7.4	120.7	8.54	0.019	27.08	27.03	21.61
231706	34.26	8.5	8.3	6.76	5.8	5.32	23.9	6.4	6.6	126.8	10.51	0.017	26.70	27.09	21.52
231707	34.20	6.2	5.1	4.22	3.9	3.16	25.6	11.9	12.2	112.2	7.95	0.021	26.87	26.69	21.43
231708	37.22	4.2	6.5	5.55	1.3	1.53	23.2	6.3	6.0	65.5	5.70	0.007	26.55	26.92	21.45
231709	35.12	7.0	5.2	4.82	2.7	3.49	23.0	nm	nm	106.8	9.62	0.012	26.57	26.70	21.90
231710	36.79	0.1	0.8	0.77	0.4	0.59	21.2	nm	nm	79.7	12.29	0.002	26.66	26.91	21.82
231711	37.50	0.4	0.9	0.69	0.6	0.59	20.4	nm	nm	57.3	5.51	nm	26.76	26.77	21.82
231712	35.31	0.2	1.3	1.21	0.6	0.25	21.5	nm	nm	56.4	5.38	0.002	26.78	26.97	21.96
231713	35.91	5.9	6.2	3.13	1.5	1.47	23.3	nm	nm	93.9	8.47	0.030	26.73	26.62	21.92
231714	37.29	2.4	2.9	1.15	0.7	0.65	30.2	3.6	3.6	113.1	22.90	0.016	26.62	26.86	22.04
231715	36.98	0.1	0.1	1.24	0.6	0.69	44.4	3.1	2.5	72.0	14.06	0.030	26.83	26.72	21.79
231716	37.28	1.6	1.6	0.59	0.4	0.71	43.0	11.2	8.3	79.5	17.77	0.001	26.91	27.06	21.84
231717	35.74	3.6	0.7	0.62	0.2	0.56	19.3	BDL	BDL	61.5	5.69	0.065	26.89	27.15	22.14
231718	37.47	0.7	0.5	0.84	0.5	0.29	19.6	BDL	BDL	57.4	5.10	0.004	27.01	26.95	21.88
231719	37.32	0.2	0.3	0.69	0.3	0.52	39.6	BDL	BDL	63.1	7.20	0.002	26.77	27.06	22.01
231720	37.64	0.4	0.5	0.80	0.9	0.27	21.3	BDL	BDL	56.9	5.55	0.005	26.86	26.91	22.01
231721	0.10	nm	nm	nm	0.2	0.64	BDL	BDL	BDL	26.8	7.24	0.008	26.67	nm	21.94
231801	31.13	9.5	9.3	8.19	10.5	8.35	22.4	11.2	14.0	184.6	13.82	0.036	nm	29.02	20.98
231802	35.01	5.3	6.5	6.03	7.0	6.25	16.4	8.6	9.4	115.9	9.45	0.019	29.76	28.30	20.88
231803	19.23	8.5	8.7	7.82	9.1	7.50	13.6	23.1	29.3	402.5	23.54	0.091	28.59	29.47	22.26
231804	21.72	10.5	11.0	9.64	10.2	8.74	35.2	22.6	26.0	356.0	20.24	0.073	28.41	28.60	22.40
231805	37.30	2.9	1.5	1.78	1.3	1.33	19.3	3.5	2.7	61.2	7.36	0.039	28.36	28.26	22.79

231806	37.23	1.1	1.4	1.86	0.6	0.73	47.6	4.3	3.7	58.7	6.41	0.011	27.38	28.20	22.59
231807	37.53	0.4	0.5	0.81	0.9	0.73	48.4	9.2	7.8	54.8	4.98	0.031	27.33	27.47	20.89
231808	36.72	0.1	0.4	0.83	1.1	1.01	29.8	10.3	8.0	53.6	5.03	0.053	27.63	27.30	22.35
231809	37.29	0.2	0.4	0.69	0.8	0.73	34.2	9.6	8.1	53.6	5.09	0.015	26.82	27.70	20.87
231810	37.55	0.1	0.3	0.73	0.6	0.47	33.8	11.0	8.8	54.4	4.85	0.006	27.10	26.92	22.34
231811	37.42	0.1	0.3	0.66	0.1	0.31	31.6	9.8	8.3	54.3	6.57	0.003	26.79	27.40	20.87
231812	37.49	0.1	0.3	0.79	0.9	0.85	35.8	8.9	8.2	53.7	6.28	0.013	27.40	26.92	20.96
231813	37.05	0.1	1.2	0.33	0.5	0.42	41.4	9.2	7.5	52.9	5.25	0.003	26.88	27.55	22.37
231814	37.42	0.1	0.8	0.58	0.7	0.44	28.4	9.0	7.7	53.2	4.59	0.020	27.52	27.19	22.49
231815	37.47	1.5	0.4	0.95	0.5	0.48	26.8	8.9	7.7	54.7	6.65	0.006	27.44	27.72	20.86
231816	37.42	0.1	1.1	0.77	0.4	0.39	39.2	8.6	7.2	54.1	6.71	0.005	26.88	27.62	22.23
231817	36.90	0.5	1.2	0.44	0.5	0.69	29.6	8.9	7.7	56.4	6.17	0.003	26.83	27.29	20.82
231818	37.64	0.2	0.3	0.60	0.8	0.96	41.4	8.7	7.9	55.1	6.27	0.010	26.94	27.06	20.89
231819	37.46	0.1	0.3	0.53	1.2	0.59	35.4	6.9	6.6	52.7	5.73	0.006	26.75	27.19	20.97
231820	36.64	0.1	0.8	0.73	0.4	0.82	19.8	6.5	5.2	51.0	4.55	0.005	27.76	26.90	22.53
231821	0.10	nm	0.0	0.29	0.7	0.86	BDL	3.7	3.3	2.8	3.66	0.006	nm	27.76	21.03